Cell Reports Sustainability

CellPress
OPEN ACCESS

Review

Renewable production of nylon precursors from lignin

Kaile Li,[1,7] Shijie Yu,[1,7] Alexandra Radu,[6] Yongqing Xu,[1] Juniza Md Saad,[2] Badr A. Mohamed,[3] Qinghai Li,[1,4] Yanguo Zhang,[1,4,*] Zhicheng Luo,[5,*] and Hui Zhou[1,4,*]

[1]Key Laboratory for Thermal Science and Power Engineering of Ministry of Education, Beijing Key Laboratory of CO2 Utilization and Reduction Technology, Department of Energy and Power Engineering, Tsinghua University, Beijing 100084, P.R. China
[2]Department of Science and Technology, Universiti Putra Malaysia Bintulu Sarawak Campus, Bintulu, Sarawak 97008, Malaysia
[3]Department of Agricultural Engineering, Cairo University, Giza, Egypt
[4]Shanxi Research Institute for Clean Energy, Tsinghua University, Taiyuan, Shanxi 030000, P.R. China
[5]MOE Key Laboratory of Energy Thermal Conversion & Control, School of Energy and Environment, Southeast University, Nanjing 210096, P.R. China
[6]Laboratory of Inorganic Materials and Catalysis, Department of Chemical Engineering and Chemistry, Eindhoven University of Technology, Eindhoven, the Netherlands
[7]These authors contributed equally
*Correspondence: zhangyg@tsinghua.edu.cn (Y.Z.), zluo@seu.edu.cn (Z.L.), huizhou@tsinghua.edu.cn (H.Z.)
https://doi.org/10.1016/j.crsus.2025.100344

SUMMARY

Cyclohexanone and cyclohexanol are critical monomeric precursors in the production of nylon 6 and nylon 66, which are conventionally sourced from petroleum. To reduce the reliance on fossil resources and embrace green chemistry, there is a need to shift to more sustainable feedstocks such as lignin, an abundant aromatic biopolymer. To convert lignin-derived monomers obtained by deconstruction of the polymer into nylon precursors, a selective hydrodeoxygenation (SHDO) step, i.e., demethoxylation and dearomatization, toward cyclohexanone and cyclohexanol needs to be carried out. However, catalytic processes required for this transition, spanning catalyst activity, stability, and product selectivity, remain uncertain. This review delves into recent strides with metal-based catalysts (e.g., ruthenium [Ru], nickel [Ni], and cobalt [Co]) on diverse supports (e.g., metal oxides and carbon materials), exploring reaction conditions (solvent, temperature, and H_2 pressure) and proposed mechanisms. It concludes by outlining catalyst challenges and future perspectives for the SHDO reaction, paving the way for sustainable nylon precursor synthesis from lignin.

INTRODUCTION

Nylon 6 and 66, high-demand polymers, currently rely on fossil resources to produce monomeric precursors such as cyclohexanone (CHN) and cyclohexanol (CHL) (Figure 1A). Conventional methods involve oxidation of cyclohexane (route 1), hydration of cyclohexene (route 2), and hydrogenation of phenol (route 3), where the precursors are predominantly sourced from petroleum, exacerbating climate change concerns.[1] A viable, sustainable alternative is to derive these raw materials from lignin, the largest natural source of aromatics.[2,3] This enhances the circular economy and reduces environmental impact through the biorefinery model.

Lignin, composed of guaiacyl (G), syringyl (S), and p-hydroxyphenyl (H) units, is increasingly available as a byproduct from the pulp and paper and bioethanol industries. These units are linked by various C–O–C and C–C bonds, such as β-O-4, α-O-4, and β-5 linkages, which contribute to its complex and heterogeneous structure.[9] This diversity, along with the high bond energy of β-5, makes selective depolymerization difficult, including low product selectivity and high energy consumption. In addition, the functional group complexity and occurrence of side reactions like repolymerization complicate the refining process, leading to difficulties in achieving controlled reactions.[10] The current practice of combusting the lignin only leads to the recovery of the heating value.[11] However, lignin depolymerization can be achieved via several methods such as pyrolysis, hydrolysis, oxidation, catalytic hydrogenolysis, and enzymatic depolymerization, which produces lignin-derived monomers (LDMs), including phenols, guaiacol, and syringol.[12–14] While pyrolysis and oxidation are effective, they often produce complex mixtures of products and byproducts. Hydrolysis, while useful, requires harsh conditions. Enzymatic depolymerization offers high specificity but suffers from slow reaction rates and limited scalability. By contrast, catalytic hydrogenolysis stands out for its milder reaction conditions and higher monomer yields, producing fewer byproducts, which simplifies subsequent refining to higher-value chemicals. Selective hydrodeoxygenation (SHDO) of LDMs enables the selective removal of oxygen-containing groups (e.g., hydroxyl and methoxy) to produce sustainable high-value compounds such as cyclohexanone and cyclohexanol.[4] Among all LDMs, guaiacol contains both hydroxyl and methoxy groups, making it an excellent representative. Considering the SHDO of guaiacol to cyclohexanol, multiple reactions are involved, including

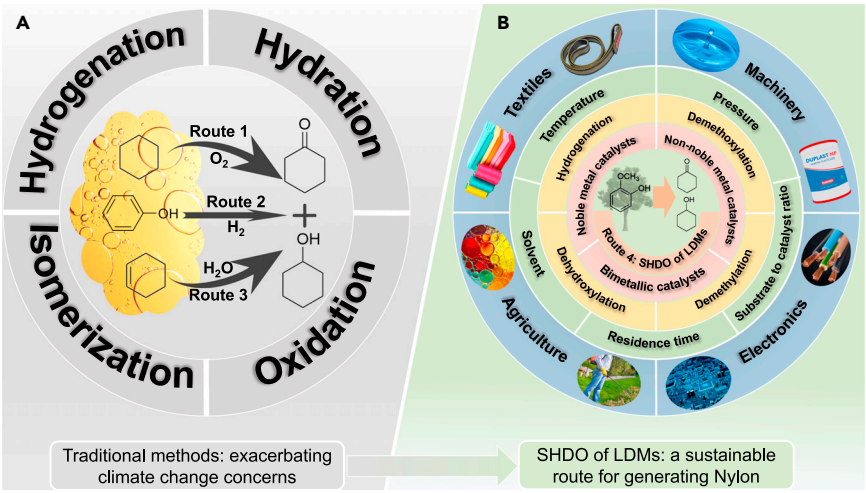

Figure 1. Current synthesis approaches from fossil fuels and SHDO approach from renewable lignin

(A) Current synthesis approaches of cyclohexanone and cyclohexanol from fossil fuels (route 1, 2, and 3).[1]

(B) SHDO approach from renewable lignin (route 4).[4–8]

hydrogenation (aromatic ring) and hydrodeoxygenation (hydrodemethoxylation and hydrodehydroxylation) (route 4 in Figure 1B). Contrary to the petroleum-based process involving fewer steps, primarily hydrogenation and oxidation, this multistep pathway places greater emphasis on reaction selectivity and catalyst stability.

Developing highly selective catalytic systems for the production of cyclohexanol has become increasingly important, particularly in addressing key challenges such as the selective retention of hydroxyl groups and preventing excessive deoxygenation, which can result in undesired byproducts like cyclohexane. The specific reaction pathways of LDMs during the SHDO reactions depend heavily on the type of metal catalyst, the nature of the support, and the reaction conditions (solvent, temperature, H_2 pressure, and reaction time). Generally, oxygen-containing groups are activated at the metal sites or the metal-support interface, while hydrogen is adsorbed and activated at the metal sites. The type of catalyst is the primary factor influencing the reaction pathways, typically involving heterogeneous catalysts, which are usually composed of transition metals (e.g., ruthenium [Ru], Pd, and nickel [Ni]).[15–20] Notably, supports with tunable acidic or basic sites (e.g., SiO_2 and Al_2O_3[21,22]) or oxygen affinity (e.g., ZrO_2, CeO_2, and TiO_2[23–26]) are also crucial. However, catalysts with high oxophilicity or hydrogenation capabilities lead to the formation of byproducts such as cyclohexane or 2-methoxycyclohexanol, highlighting the importance of appropriate metal-support interaction.[27] In addition, many catalysts suffer from deactivation due to low hydrothermal stability, coke deposition, or sintering, which underscores the need for more robust and durable catalytic systems. Enhancing LDM conversion and selectivity to nylon precursors under milder conditions, including lower temperatures and pressure and shorter reaction times, is imperative.

To the best of our knowledge, a systematic and critical review of SHDO of LDMs to cyclohexanone and cyclohexanol is currently lacking, which hinders further large-scale development. In this regard, we highlight the latest advances in catalytic systems for the sustainable production of cyclohexanol from guaiacol via SHDO, with a focus on reaction mechanisms and the development of efficient catalysts (Figure 1B). In addition, we thoroughly discuss how operational conditions, such as solvent choice, temperature, H_2 pressure, and reaction time, impact catalytic activity. Moreover, we emphasize the challenges in this field, offering preliminary suggestions and outlining future directions. We believe that this comprehensive overview will provide valuable insights for designing high-performance catalysts and advancing the production of renewable chemicals.

CATALYSTS

Ru-based catalysts

Ru-based catalysts have been shown to be very active and selective for the conversion of LDMs to cyclohexanols.[28,29] Among them, Ru/C catalysts were extensively studied for the SHDO of methoxyphenols to cyclohexanol.[30–33] Despite their high specific surface area, carbon supports are generally unsatisfactory in terms of selectivity toward cyclohexanol, because the surface lacks sites with pronounced acidic or basic properties, and also lacks effective sites for the adsorption of aromatics.[34–36] The addition of basic substances was shown to improve the conversion of methoxyphenols. For example, a Ru/C catalyst combined with MgO could selectively convert guaiacol into cyclohexanol under mild conditions (160°C, 1.5 MPa H_2, 120 min) (Figure S1A).[37] More importantly, the catalyst also exhibited a good performance for other methoxyphenolic compounds, such as 3-methoxyphenol or 4-methoxyphenol (Table 1, entries 1–4). By investigating the reactivity of intermediates, i.e., 2-methoxycyclohexanol and phenol, over Ru/C + MgO and Ru/C catalysts, MgO was indicated to suppress unselective C-O dissociation and enhance the demethoxylation to phenol. However, MgO was not stable during the reaction in the presence of water solvent. The replacement of MgO with other metal (e.g., Mn, Fe, and cobalt [Co]) showed that the yield of cyclohexanol with Ru-MnO_x/C was nearly identical to those of Ru/C + MgO (Table 1, entries 5–8).[38] The introduction of moderate basic sites suppressed the unwanted hydrodeoxygenation of cyclohexanol to cyclohexane (Figure S1B). The used Ru-MnO_x/C catalyst remained in a powdery form, exhibiting a significant improvement in reproducibility compared with the Ru/C + MgO.

ZrO_2-La_2O_3 is reported to possess medium-strength basic sites with high stability.[43,44] Ru/ZrO_2-La$(OH)_3$ catalysts with different Zr/La molar ratios (4, 2, or 1) were synthesized by a precipitation method and their SHDO performance was explored in

Table 1. SHDO of LDMs to cyclohexanols using Ru-based catalysts

Entry	Reactant	Catalyst	Solvent	Reaction conditions	Conv. (%)	CHL selectivity (%)	Ref.
1	guaiacol	Ru/C + MgO	H_2O	160°C, 1.5 MPa, 120 min	98	79	Nakagawa et al.[37]
2	3-methoxyphenol	Ru/C + MgO	H_2O	160°C, 1.5 MPa, 120 min	>99	85	Nakagawa et al.[37]
3	4-methoxyphenol	Ru/C + MgO	H_2O	160°C, 1.5 MPa, 120 min	>99	55	Nakagawa et al.[37]
4	syringol	Ru/C + MgO	H_2O	160°C, 1.5 MPa, 120 min	>99	69	Nakagawa et al.[37]
5	guaiacol	Ru + MnO_x/C	H_2O	160°C, 1.5 MPa, 240 min	>99	81	Ishikawa et al.[38]
6	3-methoxyphenol	Ru + MnO_x/C	H_2O	160°C, 1.5 MPa, 120 min	>99	76	Ishikawa et al.[38]
7	4-methoxyphenol	Ru + MnO_x/C	H_2O	160°C, 1.5 MPa, 120 min	>99	56	Ishikawa et al.[38]
8	syringol	Ru + MnO_x/C	H_2O	160°C, 1.5 MPa, 120 min	>99	70	Ishikawa et al.[38]
9	guaiacol	Ru/ZrO_2-La$(OH)_3$	H_2O	200°C, 4 MPa, 240 min	>99	92	Xu et al.[39]
10	guaiacol	Ru/Al_2O_3-acidic	cyclohexane	225°C, 1 MPa, 60 min	>99	77	Singh and Dhepe[40]
11	guaiacol	Ru/Al_2O_3-basic	cyclohexane	225°C, 1 MPa, 60 min	>99	64	Singh and Dhepe[40]
12	guaiacol	Ru/SiO_2-Al_2O_3	cyclohexane	225°C, 1 MPa, 60 min	68	0	Singh and Dhepe[40]
13	guaiacol	Ru-hTiO_2[a]	H_2O	160°C, 1.5 MPa, 100 min	>99	81	Han et al.[41]
14	guaiacol	Ru-TiO_2@SiO_2[b]	H_2O	160°C, 1.5 MPa, 100 min	>99	77	Han et al.[41]
15	guaiacol	Ru-TiO_2-eSiO_2[c]	H_2O	160°C, 1.5 MPa, 100 min	>99	84	Han et al.[41]
16	3-methoxyphenol	Ru-TiO_2-eSiO_2	H_2O	160°C, 1.5 MPa, 100 min	>99	91	Han et al.[41]
17	guaiacol	Ru/CeO_2-S	H_2O	200°C, 1 MPa, 360 min	>99	>99	Zhang et al.[42]
18	3-methoxyphenol	Ru/CeO_2-S	H_2O	200°C, 1 MPa, 360 min	>99	>99	Zhang et al.[42]
19	4-methoxyphenol	Ru/CeO_2-S	H_2O	200°C, 1 MPa, 360 min	>99	>99	Zhang et al.[42]
20	syringol	Ru/CeO_2-S	H_2O	200°C, 1 MPa, 360 min	>99	>99	Zhang et al.[42]

[a]The supports represent hollow TiO_2 spheres.
[b]The supports represent hollow TiO_2-coated SiO_2 spheres.
[c]The supports represent hollow TiO_2 spheres embedded with SiO_2 nanoparticles.

water.[39] A 91.6% yield of cyclohexanol was obtained from guaiacol using a Ru/ZrO_2-La$(OH)_3$ (Zr/La = 2) catalyst at 200°C for 240 min (Table 1, entry 9). Characterization revealed that Zr and La formed a mixed (hydr)oxide phase, which was beneficial for the stability of the catalysts. The extra methoxy group in syringol as compared with guaiacol made demethoxylation much more challenging, resulting in a decrease in the cyclohexanol selectivity.

Despite many studies demonstrating that basic supports are favorable in steering product selectivity toward cyclohexanol, moderate acidic sites are also conducive. Dhepe's group studied Ru catalysis on different supports, including SiO_2, Al_2O_3 (acidic, basic, and neutral), and SiO_2-Al_2O_3 for the conversion of guaiacol into cyclohexanol.[40] Among them, a high yield of cyclohexanol (77%) was obtained with a Ru/Al_2O_3-acidic catalyst (225°C, 1 MPa, 240 min), while a Ru/Al_2O_3-basic catalyst only exhibited a 64% yield of cyclohexanol (Table 1, entries 10–11). The authors indicated that certain adsorption of oxygenated compounds on the acidic supports was beneficial for the cleavage of aromatic C−OCH_3 bonds. However, Ru/SiO_2-Al_2O_3 with higher acidity than Ru/Al_2O_3-acidic produced no cyclohexanol, which is suggested to be associated with over-hydrogenation to cyclohexane (Table 1, entry 12). Ru catalysts supported on SiO_2, Al_2O_3, and SiO_2-Al_2O_3[45] were also investigated in the catalytic transfer hydrogenation of LDMs in isopropanol (IPA). The study suggested that Ru existed in a higher oxidation state (+2, +4) with relatively smaller particle sizes in Ru/Al_2O_3-acidic, leading to a ~74% cyclohexanol yield at 225°C and 0.7 MPa N_2 after 120 min. Acid-catalyzed dehydration of IPA to the ether became dominant over Ru/SiO_2-Al_2O_3 catalysts, resulting in a negligible conversion of guaiacol. Through density functional theory (DFT) of an adsorptive model on a Ru surface, the *cis*-isomer of 2-methoxycyclohexanol, which was more stable than the *trans*-isomer, was more likely to remain attached to the catalyst surface and hydrodeoxygenate to cyclohexanol (Figure S2).

Mesoporous materials have been widely applied in the SHDO of methoxyphenols due to their advantages in terms of mass transport.[46,47] Wang et al. fabricated Ru supported on various mesoporous TiO_2 spheres (hollow TiO_2 spheres, TiO_2-coated SiO_2 spheres, and TiO_2 spheres embedded with SiO_2 nanoparticles) for SHDO of guaiacol to cyclohexanol in an aqueous medium under relatively mild conditions (Figure S3).[41] Among them, 84.2% yield of cyclohexanol was observed using Ru-TiO_2-eSiO_2 under 160°C and 1.5 MPa H_2 for 100 min (Table 1, entries 13–16). The excellent activity was attributed to the moderate acidity of the Ru-TiO_2-eSiO_2 catalyst and its polyporous spherical structure with more active sites, which enhanced the cleavage of C–OCH_3 bonds and facilitated the reactions within the supports. Moreover, the Ru-TiO_2-eSiO_2 catalyst performed well in converting 3-methoxyphenol, which was scarcely ever converted into cyclohexanol over other catalysts due to the steric hindrance arising from the spatial arrangement of its substituents, with a selectivity of 91%.

Recently, single-atom catalysts (SACs) have attracted extensive attention for their higher dispersion of metal sites. In terms of the disproportionate dimension of the single-atom and

benzene ring, it is difficult for single atoms to meet the adsorption of benzene ring, resulting in unsatisfying SHDO activity of aromatic reactants.[48] However, oxides that contain numerous defect sites, such as corners and vacancies, exhibit variable properties (such as acidity, basicity, and redox characteristics), which may potentially aid in the adsorption of aromatic compounds. Ru single-atom centers supported on cerium dioxide with sheet morphology (Ru/CeO_2-S) were prepared using an incipient wetness impregnation (IWI) method.[42] The catalyst performed well in SHDO of guaiacol and other aromatic compounds with methoxyls substituted at the meta and para positions of the phenolic hydroxyl group into cyclohexanol with 99.9% yields (Table 1, entries 17–20). Related to the synergy between Ru single atoms and CeO_2, more oxygen vacancies were observed on the surface of Ru/CeO_2-S, which could promote the HDO of aromatics by facilitating the adsorption and transfer of the active hydrogen atoms.

Ni-based catalysts

Cost-efficient Ni-based catalysts are also found to be chemically active in facilitating the absorption of hydrogen and are widely used in hydrogenation reactions.[49] Currently, research on SHDO performance over Ni catalysts mainly focuses on support properties, preparation methods, and promoters.

Recently, Nb_2O_5 has attracted great attention due to its high hydrothermal stability and controllable structure. Ni/Nb_2O_5-PL (plates) and Ni/Nb_2O_5-Com (commercial) catalysts were synthesized by impregnation, and Ni/Nb_2O_5-PL was reported to promote SHDO of guaiacol to cyclohexanol in the aqueous phase.[50] Hierarchical Nb_2O_5 nanoplates effectively promoted the homogeneous loading of the Ni nanoparticles, and an increased number of interfacial Ni-NbO_x sites were formed by enhancing the metal-support interaction. Isotopic labeling experiments indicated that interfacial Ni-NbO_x sites could enhance the dissociation of adsorbed H_2O molecules and subsequently transfer hydrogen to adsorbed aromatics via proton transfer. Under optimized conditions (200°C, 2.5 MPa H_2, 300 min), 77% selectivity to cyclohexanol with 93.6% guaiacol conversion was obtained (Table 2, entries 1–4).

Nanoporous metals also exhibit satisfying catalytic activity under relatively mild conditions because of their numerous nanopores and active sites.[56] Over RANEY Ni, guaiacol was predominantly converted into cyclohexanol in IPA (solvent and H-donor), while 3-methoxyphenol and 4-methoxyphenol showed a high tendency of ring hydrogenation (Table 2, entry 5).[18] Another study further reported a high catalytic performance of nanoporous Ni in an aqueous medium.[51] NiAl alloy precursors prepared by several methods, namely induction melting (IM), vacuum arc melting (AM), and mechanical alloying (MA), showed that Ni-MA exhibits superior resistance to corrosion and improved stability. This approach bypasses the acid corrosion resulting from phenol generation (Table 2, entries 6–8).

Perovskite-type oxides that exhibit highly dispersed metal particles and a large oxygen storage capacity can be applied in the oxidization of coke deposits.[57] $La_{1-x}Ce_xNiO_3$ perovskite-type oxides ($0 \leq x \leq 0.9$) were prepared as precursors for Ni nanoparticles by the self-combustion method, with high activity in SHDO of guaiacol (Table 2, entry 9). It was noted that with relatively higher Ce content ($x \geq 0.5$), the absence of the perovskite structure and high dispersion of the oxide phases in an amorphous form or incorporation into CeO_2 led to high thermal stability under reductive conditions.[52] Continuous-flow reactions exhibited that the conversion changed slightly after 9 h, suggesting high stability and coke formation inhibition.

In addition to increasing the loading and dispersion of active metal sites, SHDO activity highly depends on the surface electronic density, which is affected by the acidity and basicity of the support due to electron transfer between the support and Ni particles.[58] Specifically, the basic supports donate electrons to Ni, while the acidic supports receive electrons. Long et al.[5] in their study synthesized Ni/MgO catalysts using the IWI method and subsequently investigated its performance during the SHDO reaction in decalin solvent. The doping of Ni^{2+} in the bulk lattice structure of $NiMgO_x$ weakened the interactions between Ni, Mg, and O, which further facilitated the reduction of Ni^{2+} and improved hydrogenation activity. The authors proposed that the attachment between the phenolic hydroxyl group and MgO induced the formation of an electron-rich intermediate and weakened the strength of C–OCH_3 bonds (Figure S4A). Attributed to the acid-base effect, the conversion and selectivity to cyclohexanol were both close to 100% under optimized conditions (160°C, 4 MPa H_2, 180 min) (Table 2, entry 10).

Metal-oxide supports can also increase the Lewis acidity of the catalysts, leading to high hydrogenation and hydrolysis activity.[59] Most importantly, mixed supports of CeO_2 and ZrO_2 were shown to enable the formation of metastable states that were mainly attractive for three-way catalytic (TWC) applications.[60] Recently, Ni/ZrO_2-CeO_2 catalysts were reported to exhibit good catalytic activity in the SHDO of guaiacol (Table 2, entries 11–15).[6] The addition of ZrO_2 to Ni/CeO_2 was beneficial to the thermal stability of CeO_2 and the dispersion of the Ni particles, and thus the stability of the catalyst could be improved. Besides, the introduction of ZrO_2 over Ni-based catalysts could increase the number of acidic sites, which facilitated the adsorption and activation of guaiacol molecules and modified the selectivity of products. In the presence of ZrO_2, the enhanced generation of oxygen vacancies was observed, attributed to the facile transition between Ce^{4+} and Ce^{3+} species, thereby promoting the adsorption and activation of C−O bonds in guaiacol molecules. Additionally, adding Lewis acids, such as $Al(OTf)_3$, $Sc(OTf)_2$, $Ga(OTf)_3$, $Hf(OTf)_4$, and $La(OTf)_3$, to $NiAlO_x$ materials has been proven favorable to the hydrogenolysis of highly oxygenated lignin fragments.[53] $Ni_{0.87}Al_{0.13}O_x$ with the addition of $La(OTf)_3$ exhibited 79% selectivity of cyclohexanol in IPA, while extremely low activity was observed in the absence of Lewis acids (Table 2, entries 16–20). The content of NiO increased with the addition of Al, which promoted the hydrogenolysis of the C–OCH_3 bonds. Meanwhile, Lewis acids could interact with the surface hydroxyl groups and C–O bonds of the substrates, contributing to the interaction between substrates and active sites. The authors then proposed that substrates were adsorbed on Ni nanoparticles, activated by Lewis acids, and phenol was generated by the C-O cleavage before being hydrogenated to produce cyclohexanol (Figure S4B).[53]

Catalyst preparation methods also influence the catalytic performance of metal-oxide supports. Shu et al.[54] reported

Table 2. SHDO of guaiacol to cyclohexanols using Ni-based catalysts

Entry	Reactant	Catalyst	Solvent	Reaction conditions	Conv. (%)	CHL selectivity (%)	Ref.
1	guaiacol	Ni/Nb_2O_5-PL	H_2O	200°C, 2.5 MPa, 300 min	94	77	Song et al.[50]
2	guaiacol	Ni/Nb_2O_5-Com	H_2O	200°C, 2.5 MPa, 300 min	23	27	Song et al.[50]
3	guaiacol	Ni/ZSM-5	H_2O	200°C, 2.5 MPa, 300 min	37	25	Song et al.[50]
4	guaiacol	Ni/γ-Al_2O_3	H_2O	200°C, 2.5 MPa, 300 min	55	64	Song et al.[50]
5	guaiacol	RANEY Ni	IPA	120°C, 240 min	100	95	De Castro et al.[18]
6	guaiacol	Ni-IM[a]	H_2O	180°C, 2 MPa, 240 min	94	90	Lu et al.[51]
7	guaiacol	Ni-AM[b]	H_2O	180°C, 2 MPa, 240 min	99	93	Lu et al.[51]
8	guaiacol	Ni-MA[c]	H_2O	180°C, 2 MPa, 240 min	100	90	Lu et al.[51]
9	guaiacol	$La_{0.5}Ce_{0.5}NiO_3$	n-dodecane	300°C, 5MPa, 240 min	98	51	Escalona et al.[52]
10	guaiacol	20% Ni/MgO	decalin	160°C, 4 MPa, 240 min	100	98	Long et al.[5]
11	guaiacol	Ni/CeO_2	decane	220°C, 2 MPa, 180 min	72	72	Lu et al.[6]
12	guaiacol	Ni/ZrO_2	decane	220°C, 2 MPa, 180 min	96	72	Lu et al.[6]
13	guaiacol	Ni/ZrO_2-CeO_2(1:1)	decane	220°C, 2 MPa, 180 min	99	81	Lu et al.[6]
14	guaiacol	Ni/ZrO_2-CeO_2(1:2)	decane	220°C, 2 MPa, 180 min	100	75	Lu et al.[6]
15	guaiacol	Ni/ZrO_2-CeO_2(2:1)	decane	220°C, 2 MPa, 180 min	100	81	Lu et al.[6]
16	guaiacol	$Ni_{0.87}Al_{0.13}O_x$, $La(OTf)_3$	IPA	130°C, 4 MPa, 360 min	95	79	Cui et al.[53]
17	guaiacol	$Ni_{0.87}Al_{0.13}O_x$, $Al(OTf)_3$	IPA	120°C, 4 MPa, 360 min	37	54	Cui et al.[53]
18	guaiacol	$Ni_{0.87}Al_{0.13}O_x$, $Sc(OTf)_2$	IPA	120°C, 4 MPa, 360 min	58	55	Cui et al.[53]
19	guaiacol	$Ni_{0.87}Al_{0.13}O_x$, $Ga(OTf)_3$	IPA	120°C, 4 MPa, 360 min	30	57	Cui et al.[53]
20	guaiacol	$Ni_{0.87}Al_{0.13}O_x$, Hf $(OTf)_4$	IPA	120°C, 4 MPa, 360 min	41	41	Cui et al.[53]
21	guaiacol	CP-Ni/SiO_2[d]	decalin	120°C, 2 MPa, 120 min	3	100	Shu et al.[54]
22	guaiacol	WI-Ni/SiO_2[e]	decalin	120°C, 2 MPa, 120 min	6	100	Shu et al.[54]
23	guaiacol	SS-Ni/SiO_2[f]	decalin	120°C, 2 MPa, 120 min	99	100	Shu et al.[54]
24	guaiacol	NiZr-DP/CMK-3[g]	hexadecane	300°C, 5 MPa, 480 min	99	42	López et al.[55]
25	guaiacol	NiZr-IWI/CMK-3[h]	hexadecane	300°C, 5 MPa, 480 min	100	48	López et al.[55]

[a]IM, induction melting.
[b]AM, vacuum arc melting.
[c]MA, mechanical alloying.
[d]CP, co-precipitation.
[e]WI, wet impregnation.
[f]SS, step-by-step.
[g]DP, deposition-precipitation.
[h]IWI, incipient wetness impregnation.

that step-by-step precipitated Ni/SiO_2 (SS-Ni/SiO_2) catalysts exhibited higher activity compared with ones synthesized by co-precipitation (CP-Ni/SiO_2) and wet impregnation (WI-Ni/SiO_2) (Table 2, entries 21–23). Due to the polyporous spherical structure of the SS-Ni/SiO_2 catalyst, highly dispersed Ni nanoparticles were observed both inside and outside the catalyst. The existence of appropriate acid sites and hydroxyl groups, which had a strong absorption affinity to the aromatic hydroxyl groups of guaiacol molecules, was also responsible for the significantly enhanced catalytic performance. Similarly, mesoporous carbon materials (CMK-3 and C-Cab obtained from SBA-15 and Cab-O-sil M-5 templates) supported Ni-ZrO_2 synthesized by deposition-precipitation (DP) and IWI methods were evaluated in SHDO of guaiacol.[55] Complete substrate conversion was obtained with both catalysts, whereas selectivity toward cyclohexanol varied from 42% to 48% (Table 2, entries 24–25). The IWI method favored the formation of mixed monoclinic and tetragonal phases of ZrO_2, increasing the density of acid sites of medium strength, which benefited the selectivity toward cyclohexanol.

Co-based catalysts

As a moderate oxophilic metal, Co can form strong M–O bonds with oxygen, thus reducing the energy barrier of C-OCH_3 cleavage and facilitating the deoxygenation reaction.[61] Co/TiO_2 catalysts fabricated by WI exhibited almost complete conversion of guaiacol, 3-methoxyphenol, and syringol to cyclohexanol (Table 3, entries 1–3).[20] The discovery of a TiO_y layer suggested that a strong metal-support interaction (SMSI) was responsible for the enhancement of C-OCH_3 cleavage and hydrogenation activity. By contrast, the selectivity toward cyclohexanol from 4-methoxyphenol was extremely low (Table 3, entry 4), indicating that Co/TiO_2 could only cleave the C–OCH_3 bonds efficiently with the methoxy groups substituted in the ortho-position. However, this matter requires further investigation.

Table 3. SHDO of LDMs to cyclohexanols using Co-based catalysts

Entry	Reactant	Catalyst	Solvent	Reaction conditions	Conv. (%)	CHL selectivity(%)	Ref.
1	guaiacol	Co/TiO_2	dodecane	200°C, 1 MPa, 180 min	>99	98	Liu et al.[20]
2	3-methoxyphenol	Co/TiO_2	dodecane	200°C, 1 MPa, 240 min	>99	98	Liu et al.[20]
3	syringol	Co/TiO_2	dodecane	200°C, 1 MPa, 360 min	>99	>99	Liu et al.[20]
4	4-methoxyphenol	Co/TiO_2	dodecane	200°C, 1 MPa, 480 min	>99	7	Liu et al.[20]
5	eugenol	CoNx@NC-650	dodecane	200°C, 2 MPa, 120 min	>99	>99	Liu et al.[62]
6	guaiacol	Co/C@N	hexane	220°C, 2 MPa, 360 min	56	74	Song et al.[63]
7	3-methoxyphenol	Co/C@N	hexane	220°C, 2 MPa, 360 min	>99	93	Song et al.[63]
8	guaiacol	$0.2Co_{1\text{-}NPs}$@NC	*n*-octane	180°C, 0.5 MPa, 180 min	>99	97	Wang et al.[64]

Chemical doping of carbon materials has been proposed for regulating support basicity.[65] Liu et al. prepared CoN_x@NC (nitrogen-doped carbon) by copyrolysis of cellulose and $Co(NO_3)_2$ under an ammonia atmosphere, with the catalytic activity being evaluated in the SHDO of eugenol.[62] In the presence of Co, the carbon structure changed greatly and led to the formation of pores, and the CoN_x@NC pyrolyzed at 650°C showed the highest activity in dodecane with numerous quaternary-type nitrogen and Co–N bonds (Figures S5A and S5B). Prior to aromatic ring hydrogenation, highly selective cleavage of C–OCH_3 bonds was observed under mild conditions (200°C, 2 MPa H_2, 120 min) (Table 3, entry 5). However, the high demand for ammonia and the instability of these systems hinder their application. Co/C@N catalysts simply synthesized by pyrolysis of ZIF-67, a kind of Co-containing metal-organic framework (MOF) precursor with high contents of carbon and nitrogen, turned out to be a cost-effective and environmentally friendly option.[63] MOFs, with high specific surface areas and precise pore structures, can serve as excellent processors by providing uniformly dispersed active sites.[66] Co/C@N showed excellent activity for the selective cleavage of C–OCH_3 bonds, and 3-methoxyphenol was almost completely transformed into cyclohexanol (Table 3, entries 6–7). Meanwhile, the dual-size *n*$Co_{1\text{-}NPs}$@NC catalyst derived from MOF was developed by temperature-programmed pyrolysis of *n*Co/MOF under N_2 flow and performed well in the SHDO of guaiacol (Table 3, entry 8).[64] The carbonization of N-containing ligands facilitated the formation of N-coordinated single-atom structures (Co-N_x), and the addition of Zn effectively improved Co NPs dispersion. During the sequential conversion of guaiacol to cyclohexanol, the dissociation of hydrogen was primarily observed on Co NPs, and Co single atoms played a crucial role in the highly selective cleavage of the C–OCH_3 bond, further confirmed by DFT. The energy barrier of hydrogen dissociation over Co (111) was almost half of Co-N_4, and the energy barrier of C–OCH_3 bond cleavage in the case of Co-N_4 was lower than that of Co(111) (Figures S5C and S5D).

Bimetallic catalysts

Compared with monometallic catalysts, the addition of a second metal can increase the amount and dispersion of active metal sites. With that, the electronic and geometric properties are modified, thereby enhancing catalytic activity and selectivity through synergistic and bifunctional effects.[67–69] Bimetallic catalytic systems were reported in the oxidation, hydrogenation, and catalytic reforming of biomass to produce hydrogen,[70] alcohols,[71] and carbonylic acids.[72] Recently, bimetallic catalysts of great development potential have also been investigated in SHDO of LDMs to cyclohexanol.

It was previously believed that the introduction of Co was beneficial for the improvement of the dispersion and stability of active sites in phenol hydrogenation.[73] Hence, Ni-Co bimetallic catalysts have been applied for SHDO of guaiacol to cyclohexanol. Ni and/or Co supported on γ-Al_2O_3 and ZSM-5 were examined for SHDO of guaiacol at relatively milder conditions, and the highest selectivity toward cyclohexanol (70.9%) was obtained over (10 + 10)% NiCo/γ-Al_2O_3 in an aqueous medium in

Table 4. SHDO of LDMs to cyclohexanols using bimetallic catalysts

Entry	Reactant	Catalyst	Solvent	Reaction conditions	Conv. (%)	CHL selectivity (%)	Ref.
1	guaiacol	NiCo/ZSM-5	H_2O	200°C, 5 MPa, 480 min	71	13	Zhou et al.[74]
2	guaiacol	NiCo/γ-Al_2O_3	H_2O	200°C, 5 MPa, 480 min	96	71	Zhou et al.[74]
3	guaiacol	Ni/γ-Al_2O_3	H_2O	200°C, 5 MPa, 480 min	76	41	Zhou et al.[74]
4	guaiacol	Co/γ-Al_2O_3	H_2O	200°C, 5 MPa, 480 min	85	46	Zhou et al.[74]
5[a]	guaiacol	NiCo/CNT	IPA	220°C, 2 MPa, 120 min	>99	94	Chen et al.[75]
6	guaiacol	Ru-Co/C-600	n-decane	200°C, 1 MPa, 180 min	>99	94	Xu et al.[76]
7	4-propylguaiacol	$RuCoN_x$/NC	n-dodecane	220°C, 1 MPa, 240 min	>99	92	Zhao et al.[77]
8	guaiacol	$RuCoN_x$/NC	n-dodecane	220°C, 1 MPa, 240 min	>99	89	Zhao et al.[77]
9	syringol	$RuCoN_x$/NC	n-dodecane	220°C, 1 MPa, 240 min	32	66	Zhao et al.[77]
10[a]	guaiacol	Ni-Mn/Nb_2O_5	H_2O + IPA	220°C, 1 MPa, 300 min	56	74	Tong et al.[78]

[a]Nitrogen as the gaseous medium.

comparison with monometallic catalysts (Table 4, entries 1–4).[74] Based on this, the addition of Co to Ni/γ-Al_2O_3 facilitated the formation of highly dispersed catalysts with small metal particle sizes and enhanced the interaction between metal species and support, which would improve the catalytic activity. In addition, γ-Al_2O_3 with appropriate acidity could inhibit the dehydration of cyclohexanol to cyclohexane and increase catalytic activity compared with ZSM-5. Following this, carbon nanotube (CNT)-supported catalysts with different loadings of Ni and/or Co as active metals were synthesized by impregnation, and the SHDO of guaiacol was conducted employing IPA as the hydrogen source.[75] Bypassing the use of hydrogen reduces production costs, and the byproducts such as 2-methoxycyclohexanol were suppressed. The (15% + 5%) NiCo/CNT provided the highest conversion of guaiacol (100%) with cyclohexanol as the main product (94%) (Table 4, entry 5).

The synthesis of Ru-Co bimetallic catalysts could fully exploit the properties of Ru and Co to serve as moderate oxophilic metals to improve catalytic activity. For example, a carbon-supported Ru-Co bimetallic catalyst was synthesized via CP and a glucose-induced hydrothermal method (Ru-Co/C-600, reduced at 600°C), and it showed high selectivity (~94%) and reusability in the SHDO of guaiacol (Table 4, entry 6).[76] Attributed to the highly dispersed Ru/Co sites, the dissociation of molecular hydrogen and hydrogen transfer was promoted. Additionally, the abundant oxygen vacancies were beneficial for the adsorption and activation of the methoxy group in phenolic compounds. Another N-doped bimetallic $RuCoN_x$/NC catalyst was prepared via direct pyrolysis of chitin impregnated with precursors of Ru and Co. This catalyst afforded excellent catalytic activity in SHDO of 4-propylguaiacol and guaiacol, whereas syringol obtained only 32.3% conversion due to more pronounced steric hindrance (Table 4, entries 7–9).[77] In the presence of bimetallic precursors, the development of porous structures and the inhibition of particle growth were observed, which led to highly developed micro-mesoporosity and dispersed metallic particles. This way, phenolic compounds were more likely to be absorbed on the active sites; hence, the dissociation of the C−O bonds occurred easily. Furthermore, Co exhibited enhanced dissociation of hydrogen due to electron transfer from Ru to Co, and the electron-enriched pyrrolic-N and pyridinic-N were also thought to be responsible for this improvement in the adsorption ability and the catalytic performance.

In addition to Co, a series of transition metals (e.g., Mn, Zr, Cu, and Mo) were co-supported on Nb_2O_5 with Ni for SHDO of guaiacol using alcohol as the hydrogen donor under nitrogen atmosphere.[78] Among them, the Ni-Mn/Nb_2O_5 catalyst with higher dispersion of metal particles, better specific surface area, and larger amounts of medium-strength acid sites showed the best catalytic activity (Table 4, entry 10). In addition, the catalyst exhibited good applicability in SHDO of m-cresol and 3-methoxyphenol, which could be efficiently converted to cyclohexanol.

Overall, Ru-based catalysts supported on oxides with tunable acidic/basic sites or oxygen affinity show great promise in improving selectivity and suppressing byproducts, although the high cost and scarcity of Ru remain challenges for large-scale application. Sustainability can be improved by developing more durable catalysts or using systems with lower Ru loadings, as well as employing regeneration techniques such as thermal or solvent-based methods to restore catalytic activity. For non-noble metal catalysts, despite requiring harsher reaction conditions, they can exhibit good activity under milder conditions when hydrogen-donating solvents like IPA are used, reducing energy consumption and improving industrial applicability. Solvent recovery and recycling methods, including distillation and extraction, are critical for minimizing environmental impact and ensuring the sustainability of these processes. Additionally, bimetallic catalysts offer synergistic effects and enhanced stability, especially when non-precious metals are incorporated, which not only boosts catalytic performance but also facilitates the use of greener solvents, presenting a sustainable and effective strategy for future research.

REACTION CONDITIONS

The above discussions have concentrated on the physical and chemical properties of the catalysts influenced by the interaction between active metals and supports. However, the catalytic conversion of LDMs into cyclohexanols can be extensively influenced by operational conditions, including solvent, temperature, pressure, and reaction time. Hence, a more thorough comprehension of the effect of process conditions on catalytic activity is crucial to optimize SHDO and maximize cyclohexanol yields.

Solvent

In heterogeneous catalytic systems, the interaction between catalysts, solvents, and substrates is significant for evaluating the potential of reactions. Previous work has concluded the main functions of solvents: (1) dissolving reactant(s), (2) providing the liquid phase environment for the interaction of substrates and catalysts, and (3) participating directly in reactions through interactions with substrates or catalysts.[79,80] In the past few years, many efforts have been devoted to investigating the effect of solvents on the SHDO of LDMs.[81–85] In addition to performance and compatibility, it is crucial to consider the sustainability of solvents. The environmental impact, such as toxicity, biodegradability, and availability of solvents, plays an increasingly important role in the overall efficiency and sustainability of catalytic processes.

Solvents can significantly influence catalytic activity by altering the adsorption strength of intermediates through adsorbate-solvent and metal-adsorbate interactions, which in turn change the activation energy and reaction free energy.[79] As mentioned above, due to the presence of a non-polar aromatic ring, slightly polar methoxy group, and polar hydroxyl group, guaiacol exhibits high sensitivity to solvent polarity. The presence of polar solvents facilitates solute-solvent interactions through hydrogen bonding or London forces, resulting in increased adsorption strength of guaiacol and its derivatives. For comparison, the adsorption strength decreases using non-polar solvents such as *n*-hexane.

Polar solvents generally exhibit a higher tendency to adsorb on catalyst surfaces, hindering chemisorption at active sites and activation of aromatic rings.[86] For instance, since guaiacol (29.46 $Å^2$) and water (29.27 $Å^2$) have a similar molecular polar

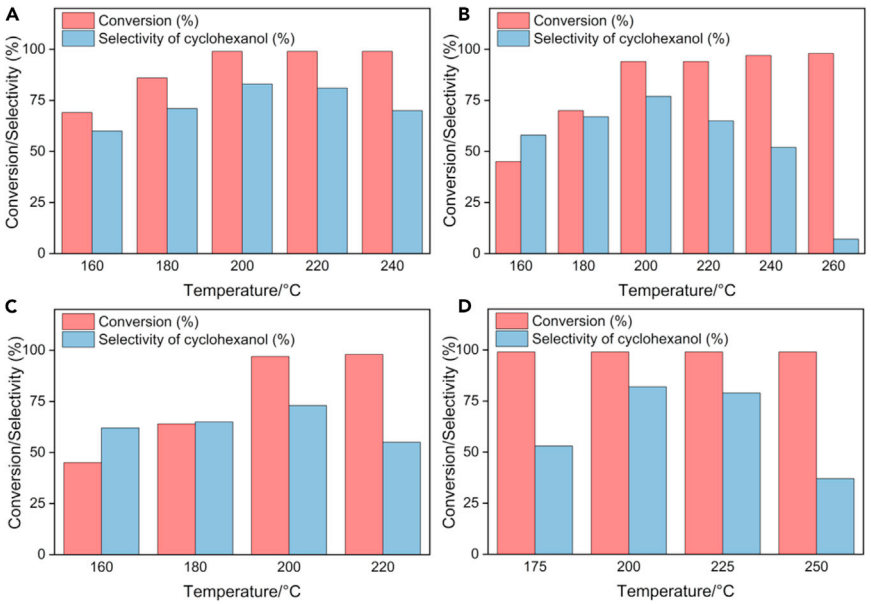

Figure 2. The effect of temperature on the cyclohexanol yield from guaiacol over

(A) Ni-Fe/$MgAlO_{x-1}$ (replotted based on the data from Huang et al.[91]), (B) Ni/Nb_2O_5 (replotted based on the data from Song et al.[50]), (C) $NiCo/Al_2O_3$ (replotted based on the data from Zhou et al.[74]), and (D) Ru/Al_2O_3 (replotted based on the data from Singh and Dhepe[40]). Reaction conditions: (A) H_2, 4.0 MPa; reaction time, 8 h; molar ratio of IPA/H_2O is 7/3. (B) H_2, 2.5 MPa; reaction time, 5 h; solvents, H_2O. (C) H_2, 5.0 MPa; reaction time, 8 h; solvents, H_2O. (D) H_2, 1.0 MPa; reaction time, 4 h; solvents, cyclohexane.

surface area, the competition between guaiacol and H_2O for interaction with the catalyst was enhanced over polar Ru/Al_2O_3 catalysts due to their concentration difference.[40] Another study has also found that the competitive adsorption over Ni sites would inhibit the aromatic activation, leading to slow hydrogenation of aromatic compounds.[86] When methanol was selected as solvent over $NiCo/\gamma\text{-}Al_2O_3$ catalyst, it was adsorbed on the active sites and underwent acetal reactions with cyclohexanone.[74] Furthermore, as an intermediate of the reaction, the addition of methanol led to chemical equilibrium movement and limited the demethoxylation reaction. By contrast, cyclohexane solvent would decrease the interactions between solvents and catalysts, which was proved to decrease further conversion of cyclohexanol and enhance the hydrogenation activity.[40] Herewith, vertical adsorption of hydroxyl groups was proposed to take precedence in polar solvents, whereas coplanar adsorption of aromatic rings followed by ring hydrogenation dominates in non-polar solvents.[84]

Fortunately, switching to other oxophilic supports (e.g., TiO_2, CeO_2, and Nb_2O_5) could significantly reduce the competitive adsorption between solvents and substrates. Based on this, absorbed H_2O molecules over catalysts were proven to transfer hydrogen to absorbed aromatic compounds via proton transfer and hence diminish the C-OCH_3 cleavage barrier by donating a proton (Figure S6A).[50] Meanwhile, another study reported that proton-assisted pathways were accomplished by developing a charge-separated $[Ru(s)\text{-}(C_6H_5O^-)\cdots(H^+)\cdots OCH_3]^\dagger$ transition state, which could decrease the barrier of C-OCH_3 cleavage by 0.8 eV (Figure S6B).[85] It was noteworthy that IPA could produce *in situ* hydrogen protons in the presence of active sites, and perform well in the removal of β-hydride.[87–89]

Temperature

In general, elevated temperature is preferred for the catalytic conversion of guaiacol into cyclohexanol, due to the enhancement of the kinetic energy of molecules. It should be noted that the hydrogenation of the aromatic ring is an exothermic reaction, while the C–O bond hydrogenolysis is an endothermic reaction.[68] Further, sufficient energy positively influences the thermodynamic and kinetic properties of the SHDO process.[90] Thereby, the opposite effects need to be balanced to obtain the optimum conversion to cyclohexanol.

Based on experiments, elevated temperature has indubitably been shown to contribute to the efficient conversion of guaiacol, and the maximum conversion was achieved at 200°C (Figures 2A–2D).[40,41,50,74,91,92] However, the selectivity of cyclohexanol initially increased until reaching a peak value with temperature increasing. Over $Ni\text{-}Fe/MgAlO_{x-1}$, with the temperature raising from 160°C to 200°C, guaiacol conversion increased from 68.9% to >99.0%, and the cyclohexanol selectivity improved from 59.6% to 82.7% under 4 MPa hydrogen for 8 h (Figure 2A).[91] Meanwhile, the selectivity toward 2-methoxycyclohexanol was decreased, indicating that higher temperatures benefit the cleavage of C-OCH_3. In addition, the conversion of guaiacol and cyclohexanol selectivity exhibited similar behavior over Ni/Nb_2O_5, $NiCo/Al_2O_3$, and Ru/Al_2O_3 (Figures 2B–2D).[40]

However, temperatures above 200°C are not generally suitable for the production of cyclohexanol in terms of both high cost and low selectivity toward cyclohexanol, which may also be unsustainable from an environmental standpoint (Figures 2A–2D). In general, there are two possible mechanisms accounting for the reduction of selectivity. Firstly, on the acid sites of the catalyst, with the increase of temperature, the formation of carbocations resulting from the dehydration of alcohol compounds leads to the formation of coke.[93] Secondly, side reactions occur at high temperatures (>200°C), which may contribute to the formation of deoxygenated products, and ~3% cyclohexane selectivity was observed at 240°C and 4 MPa H_2 over $Ni\text{-}Fe/MgAlO_{x-1}$.[40] It should be noted that the optimum temperature depends on the type of catalysts and other reaction parameters.

Hydrogen pressure

Hydrogen pressure plays an important role in SHDO reactions as the change of pressure influences the solubility of hydrogen in

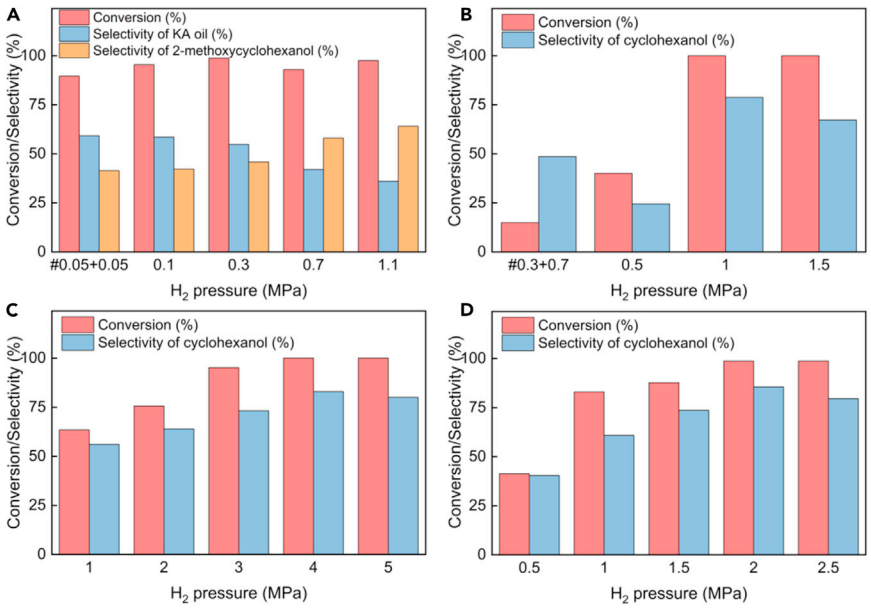

Figure 3. The effect of hydrogen pressure on the cyclohexanol yield from guaiacol over

(A) Pd/CeO_2. Replotted based on the data from Zhou et al.[24]

(B) Ru/Al_2O_3. Replotted based on the data from Singh andDhepe.[40]

(C) Ni-Fe/$MgAlO_{x-1}$. Replotted based on the data from Bykova et al.[95]

(D) Ru-MnO/AWMCNT. Replotted based on the data from Qi et al.[96] Reaction conditions: (A) Reaction temperature, 200°C; reaction time, 8 h; solvents, H_2O. (B) Reaction temperature, 200°C; reaction time, 8 h; solvents, cyclohexane. (C) Reaction temperature, 200°C; reaction time, 8 h; molar ratio of IPA/H_2O ratio is 7/3. (D) Reaction temperature, 200°C; reaction time, 200 min; solvents, decahydronaphthalene. #X + Y: X MPa partial pressure of hydrogen mixed with Y MPa partial pressure of nitrogen. AWMCNT, acidic treatment of multi-walled carbon nanotubes.

the solvent. A positive linear correlation between hydrogen solubility and pressure is exhibited at different temperatures (Figure S7). Due to the non-polarity of hydrogen, solubility in water is relatively lower than that in organic solvents with low polarity, or in mixtures of solvents.[94] Higher solubility provides better interactions between substrates and active sites of the catalyst during SHDO processes. In addition, the hydrogen serves as a reactant in SHDO reactions, which significantly impacts the reaction equilibrium and kinetics.[40]

The effect of H_2 pressure on guaiacol conversion and cyclohexanol selectivity was investigated under different reaction conditions over various supported metal catalysts (Figures 3A–3D).[7,24,40,91] Generally, an increase in pressure always enhanced the conversion of guaiacol, while the highest selectivity of cyclohexanol was obtained at 2–4 MPa hydrogen pressure in many instances (Figures 3C and 3D). However, it was reported that SHDO could be achieved even under 1 MPa pressure with high guaiacol conversion (~100%) and cyclohexanol selectivity (~80%).[40] Furthermore, lower conversion and selectivity were observed using 0.3 MPa partial pressure of hydrogen mixed with 0.7 MPa partial pressure of nitrogen (Figure 3B), indicating that the availability of hydrogen on the catalyst is more significant than the increase in interactions between the catalyst and substrate due to higher pressures. Another study reported a relatively high cyclohexanol selectivity under an unusual hydrogen pressure of 0.1 MPa and defined the total H_2 utilization efficiency and H_2 utilization efficiency for cyclohexanol and cyclohexanone (KA oil), where CHL, CHN, and MCH denoted the moles of cyclohexanol, cyclohexanone, and 2-methoxycyclohexanol, respectively (Equations 1 and 2).[24] Remarkably, selectivity for the KA oil increased with lower H_2 pressure, and the conversion of guaiacol practically remained above 90% (Figure 3A), representing higher H_2 utilization efficiency compared with other processes.

$$\text{Total } H_2 \text{ utilization efficiency} = \left(\frac{\text{CHL} \times 4+\text{CHN} \times 3+\text{MCH} \times 3}{\text{headspace } H_2+\text{dissolve}H_2}\right) \times 100\% \quad \text{(Equation 1)}$$

$$H_2 \text{ utilization efficiency for KA oil} = \left(\frac{\text{CHL} \times 4+\text{CHN} \times 3}{\text{headspace } H_2+\text{dissolve}H_2}\right) \times 100\% \quad \text{(Equation 2)}$$

Meanwhile, H_2 pressure beyond optimum reaction conditions can actually inhibit cyclohexanol formation and lead to the formation of other compounds, such as 2-methoxycyclohexanol.[24,74] A lower H_2 supply could diminish the rate of sequential H additions.[24] In such a case, the cleavage of C–O bonds became less prevalent, and hydrogenation of aromatic rings became dominant at a higher hydrogen pressure (Figure S8). In addition, the excess availability of hydrogen has been proven to promote the formation of fully deoxygenated products (i.e., cyclohexane).[50,91]

Reaction time

Increasing residence time helps the conversion of LDMs by providing sufficient time to react,[41] while shorter times are usually better for selectivity toward cyclohexanol. Shu et al.[54] reported a sharp increase in conversion when prolonging the reaction time from 1.5 to 2 h, attributed to the induction period of the heterogeneous catalyst.[97] When the reaction time is long enough, the substrates reach almost full conversion, while a further extension of time exhibits no effect on the conversion.[78] In a relatively short time, high selectivity toward fully hydrogenated and partially deoxygenated products, mainly cyclohexanol and methoxy cyclohexanol, is spotted. After an extended time, the selectivity toward cyclohexane and other side products

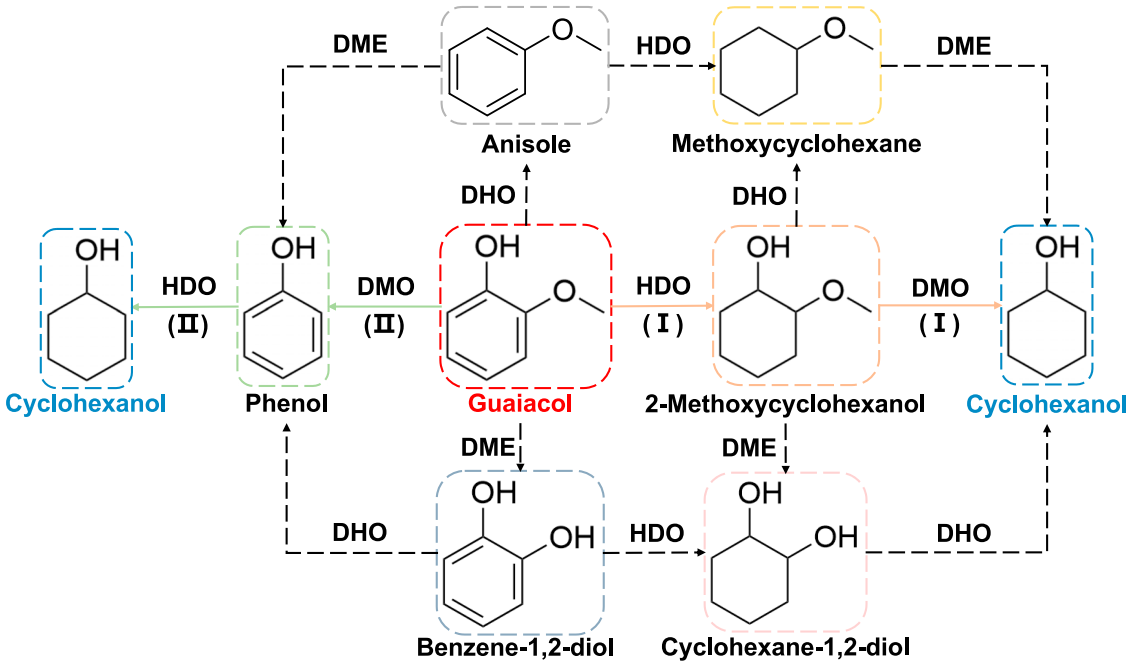

Figure 4. The possible reaction mechanisms of guaiacol to cyclohexanol
HDO, hydrogenation; DHO, dehydroxylation; DMO, demethoxylation; DME, demethylation.

increases through dehydration reactions from cyclohexanol.[2,55] Moreover, the polymerization of products and the catalyst being covered by such polymers lead to partial deactivation.[78]

Other reaction conditions, such as additions and the S/C (substrate to catalyst) ratio, are also highly important in SHDO reactions. For instance, the addition of acetic acid provided more H^+ that promoted the demethoxylation of 2-methoxycyclohexanol, thereby increasing the selectivity toward cyclohexanol.[98] Higher S/C ratio results in a deficiency of active sites, which favors side reactions. Singh et al. observed an increase in the concentration of cyclohexanol with a decrease in the S/C ratio (165–500) during the SHDO process.[40]

In summary, selecting high-efficiency solvents is essential for reducing catalyst consumption and minimizing byproduct formation. Using renewable green solvents or ionic liquids, as alternatives to traditional organic solvents, not only enhances reaction efficiency but also reduces harmful waste emissions, thereby promoting environmental sustainability. To reduce energy consumption, more efficient heating systems, such as microwave or plasma technologies, can be employed. Ensuring the recovery and reuse of heat within the process further enhances sustainability. The development of catalysts capable of operating efficiently at lower hydrogen pressures, or utilizing hydrogen from renewable sources, increases hydrogen utilization efficiency. Furthermore, adopting continuous reaction systems can shorten residence time and boost reaction efficiency. By integrating these approaches—green solvents, energy-efficient heating, optimized hydrogen usage, and process improvements—SHDO processes can achieve greater sustainability, minimizing environmental impact while maintaining high performance.

SHDO REACTION MECHANISMS

Reaction pathways

Since guaiacol is a typical LDM featuring key functional groups (aromatic ring, phenolic hydroxyl, and methoxy groups), herein, we take guaiacol as an example to discuss the SHDO reaction mechanisms of LDMs. In view of the catalysts and the effect of reaction conditions reported previously, two predominant reaction mechanisms of the SHDO reaction are proposed (Figure 4).[5–8,31,37,38,41,55] The first mechanism involves the complete hydrogenation of the benzene ring, followed by demethoxylation to cyclohexanol (pathway I). Another proposed major pathway includes the direct conversion of guaiacol to phenol via demethoxylation with subsequent hydrogenation to cyclohexanol (pathway II). Additionally, catechol is observed in some reactions, indicating a potential dehydroxylation pathway from catechol intermediates to phenol.

Upon closer inspection, steric and electronic constraints were proposed to play a significant role in the SHDO of guaiacol. Typically, the demethylation of guaiacol is more likely to occur than demethoxylation due to the relatively lower O–Me bond energy. However, Song et al. found a high preference for phenol over catechol due to steric constraints, that is, it was easier for the C–OMe bond to approach the catalyst surface.[99] Another study showed that the parallel orientation of guaiacol to the catalyst surface enabled stronger interactions between the methoxy C–O bonds and the catalyst surface, and facilitated the removal of C-OCH_3 groups.[18] By contrast, meta- and para-methoxy groups were located away from the surface due to the tilted adsorption of methoxyphenol, which weakened the interactions with the catalyst and reduced the extent of cleavage of methoxy C–O bonds.

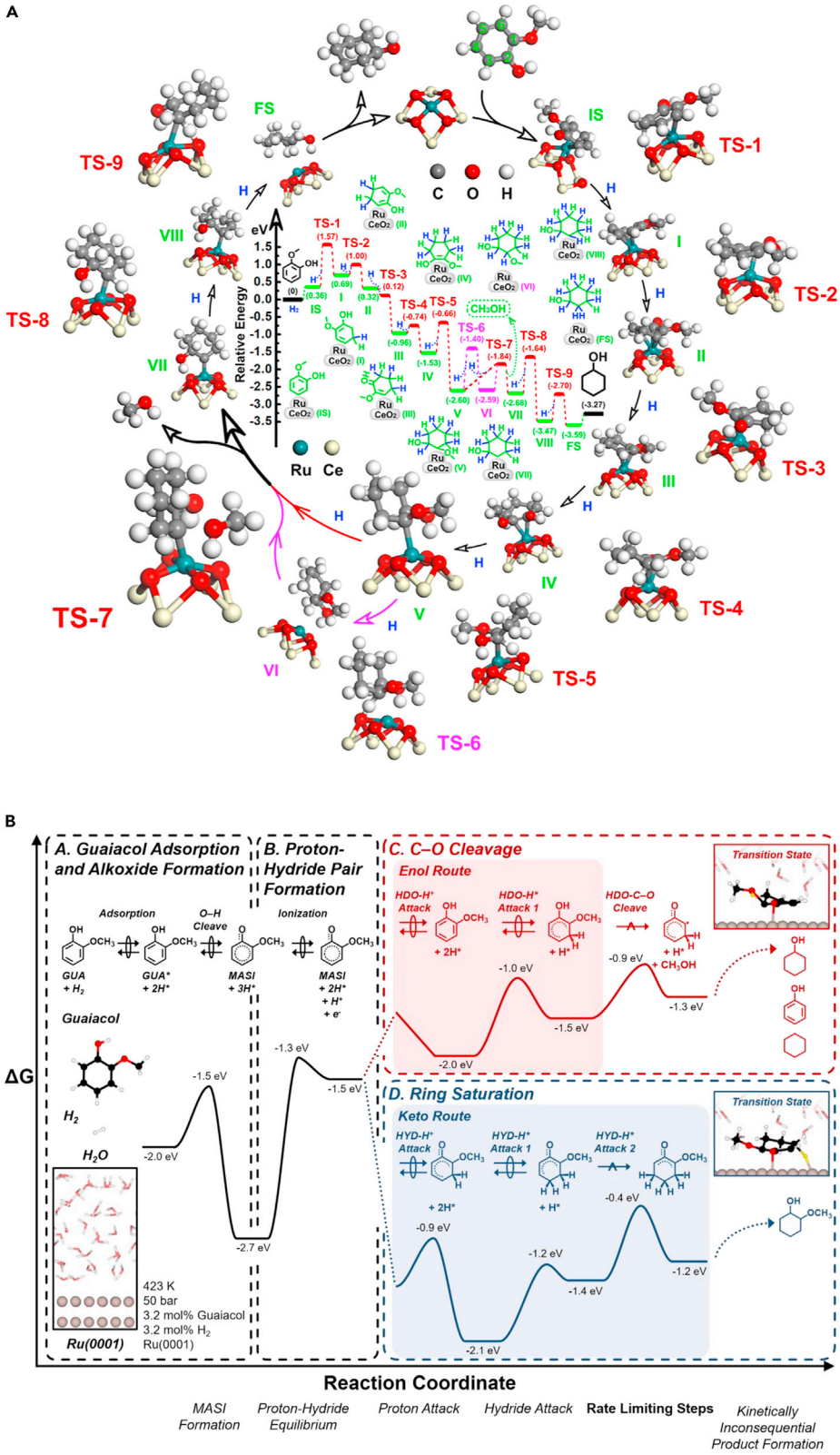

(legend on next page)

In addition, due to steric and electronic constraints, the removal of the methoxy or hydroxy functional groups is significantly faster from aromatic rings than from cyclohexane rings.[99,100] Based on results obtained using a microkinetic model, the removal of methoxy from an aromatic ring is found to be 36 times faster than that from a saturated ring, and the removal of hydroxyl from an aromatic ring is 42 times faster than that from a saturated ring.[100] The SHDO reaction activation energy of saturated reactants is also significantly higher than that of aromatic reactants, indicating that more attention should be paid to enhancing the selectivity of pathway II.

Several unique reaction pathways are distinguished by the intermediates in some research, such as 1,2-cyclohexanediol generated from the hydrogenation of catechol or hydrodemethylation of 2-methoxycyclohexanol.[50,101] In previous SHDO research on guaiacol, substantial amounts of methyl-substituted cyclohexandiol were detected, especially over bimetallic catalysts.[95,102] Migration of the methyl group to the benzene ring on the Ni sites, followed by hydrogenation to 1-methyl-1,2-cyclohexanediol was found to be responsible for such a transformation.[103] In addition, guaiacol could be reformed via hydrogenation of the aromatic ring and isomerization over a Rh catalyst at a relatively lower temperature (<150°C), with 1-methyl-1,2-cyclohexanediol being further transformed into cyclohexanol through deoxygenation.[104]

Reaction mechanism studied by DFT

Regardless of the active sites and supports of metal-based catalysts, the proposed mechanisms for the HDO of LDMs are similar. Monomer molecules are chemisorbed on the catalyst surface, forming π-complexes between the aromatic rings and active sites, whose rate largely depends on the electrostatic and steric properties of the molecules. Afterward, hydrogenation and C-OCH_3 cleavage occur, and the products are ultimately desorbed from the surface of the catalyst. Qi et al.[96] applied DFT to calculate the electrostatic potentials of the monomers and discovered that alkoxy-substituted phenol exhibited a less concentrated negative potential area that extended to the alkoxy group, due to its negative inductive effect and hyperconjugation (Table 5). The electrostatic nature is conducive to the chemisorption of the alkoxy group on the catalyst surface, enabling high SHDO to cyclohexanol.

DFT studies were developed to comprehend the active intermediates associated in the reaction pathway of the SHDO of guaiacol. Microkinetic model analysis brought to light that deoxygenation activity might decrease in the following order Ru > Rh > Pd ≈ Pt, according to the oxophilicity of transition metals.[105] Guaiacol is absorbed on Ru surface via van der Waals interactions of aromatic C atoms at the interface, and vertical physisorbed and horizontal chemisorbed sites were further looked into on the surface of Fe (110) and Pd (111).[45,106] The resulting differential charge density distributions (Figure S9) exhibited weak adsorption energy in the case of the vertical site, while most charge transfer occurred between horizontal aromatic carbon and catalyst surface. Furthermore, interactions between the hydroxyl oxygen with nearby Fe atoms on Fe (110) could also promote the removal of oxygen-containing functional groups. By contrast, the interaction between functional groups and Pd (111) active sites could be neglected, thereby enhancing the saturation of the aromatic ring.

To explicitly reveal the pathways during SHDO of LDMs, DFT calculations were performed to gain more insight into the energy profile. During the reaction, SHDO of guaiacol on Ru/CeO_2-S catalyst is thought to proceed via hydrogenation of the benzene ring with subsequent dissociation of the C–OCH_3 bond (Figure 5A).[42] Moreover, the projected density of states analysis provided more concrete analysis for the conversion of intermediates. DFT calculations were conducted to compare the Gibbs Energy of different pathways and shine light on the interaction in SHDO reaction at the H_2O-Ru(0001) interface (Figure 5B).[85] Here, the two hydrogen atoms (H*) produced from the dissociation of H_2 interact with the interface H_2O molecules and are converted into interfacial H^+ (step A and step B). Meanwhile, ketone or enol isomers produced via hydrogenation of alkoxide intermediates would carry out H^+ or H* attacks to prompt C-OCH_3 cleavage or ring saturation reaction, depending on the catalytic sequence, the recognition, and the orientation of active hydrogen (step C and step D).

CONCLUSIONS AND PERSPECTIVES

As an attractive alternative to petroleum-derived nylon precursors, lignin-derived cyclohexanone and cyclohexanol generated from the SHDO reaction of LDMs have been extensively studied and optimized for improving environmental-economic performance in recent 5 years. This review focuses on the exploration of catalyst designs, the crucial role of reaction conditions, and mechanistic investigations. After thoroughly assessing all matters, it is imperative to offer comprehensive guidance for future research in both laboratories and industries.

Hitherto, metal catalysts based on Ru, Ni, and Co have been demonstrated to exhibit excellent catalytic performance, selectivity, and recyclability, albeit with restricted commercial application. Considering the high energetic demands coupled with the high price of active metals, the SHDO reaction of LDMs is often not cost-effective. Moreover, appropriate solvent selection remains a challenge due to the complexities associated with product separation and maintaining catalyst reusability, especially for Ni-based catalysts generally tested in organic solvents (e.g., hexadecane, decalin, and n-dodecane). Bimetallic catalysts with tunable metal interactions, currently under development, could bypass the aforementioned challenges. Moving forward, the design and optimization of future catalysts should consider their entire life cycle, with greater emphasis on the improvement of catalyst efficiency, taking into account sustainability principles.

Figure 5. DFT calculation and reactive intermediates and energies

(A) DFT calculation of the reaction of guaiacol over Ru/CeO_2-S (reproduced with permission from Zhang et al,[42] Copyright 2022, ACS Publications) and (B) reactive intermediates and their energies for the two competitive pathways of C–O cleavage and ring saturation during guaiacol-H_2 reactions at the H_2O-Ru(0001) interface (reproduced with permission from Hensley et al.[85] Copyright 2021, Elsevier).

CellPress
OPEN ACCESS

Table 5. Electrostatic potentials of several LDMs

No.	Molecular formula	Electrostatic potential
1	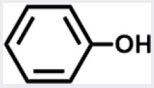	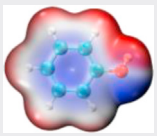
2	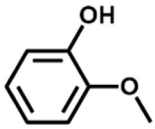	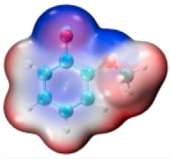
3	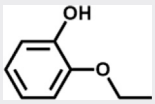	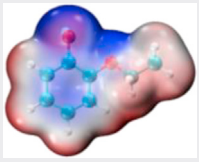
4	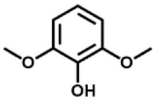	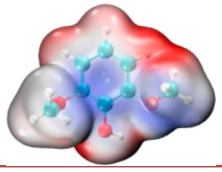

−0.03 (a.u.)

 0.03 (a.u.).

See Qi et al.[96]

As discussed in this review, catalytically relevant conditions (e.g., temperature, H_2 pressure, and time) play crucial roles in the SHDO of guaiacol, which is rarely studied in depth. Under harsh operating conditions, the properties and functions of the active sites might change. Hence, it is vital to monitor the dynamic changes in the catalyst's active sites to accurately predict and understand the deactivation process. In order to make the reaction economically feasible and sustainable, establishing an interaction framework between operational parameters is of utmost importance.

Computational investigations of in-depth analysis have rarely been executed, resulting in controversial mechanisms of the SHDO reaction of guaiacol. For example, despite the prevalent consensus that catalytic performance is determined by the interactions among active sites, supports, and solvents, the nature of active sites, detailed metal-support interactions, and the role of solvents at the molecular level as well as reaction mechanisms are still under debate. Concerning this, further theoretical and practical studies, including surface science techniques and molecular simulations like *in situ* Fourier transform infrared (FTIR) and DFT analysis, are essential for a deeper molecular understanding of the reaction. It is crucial to address the significant gap in our understanding of these catalytic systems under real operational conditions, such as high pressure and temperature, since most characterizations are done under high vacuum.

Finally, employing life cycle assessments (LCAs) and technical economic analyses (TEAs) for evaluating both the environmental impacts and costs throughout the entire production lifecycle is essential, an approach that has yet to be thoroughly explored. This evaluation spans from the collection and pretreatment of lignin, through the preparation of catalysts, to the generation of cyclohexanol, and even includes the recycling of waste catalysts. This will provide a comprehensive assessment revealing the specific environmental and economic impacts at various stages, thus facilitating the identification and optimization of key processes.

ACKNOWLEDGMENTS

The financial support from the Tsinghua-Toyota Joint Research Fund, the National Natural Science Foundation of China (grant no. 52276202), the National Key R&D Program of China (2023YFC3905701), the Beijing Natural Science Foundation (JQ24053), the Natural Science Foundation of Shanxi Province (202403021212148 and 202403021211024), the Huaneng Group Science and Technology Research Project (KTHT-U23GCZH01), the International Joint Mission On Climate Change and Carbon Neutrality, the Yunnan Major Scientific and Technological Projects (202302AQ370001), and the Tsinghua University Initiative Scientific Research Program are gratefully acknowledged.

AUTHOR CONTRIBUTIONS

Conceptualization, Q.L., Y.Z., Z.L., and H.Z.; investigation, K.L., Y.X., J.M.S., and B.A.M.; writing – original draft, K.L., S.Y., and A.R.; writing – review and editing, all authors; visualization, K.L. and S.Y.; and supervision, Z.L. and H.Z.

DECLARATION OF INTERESTS

The authors declare no competing interests.

SUPPLEMENTAL INFORMATION

Supplemental information can be found online at https://doi.org/10.1016/j.crsus.2025.100344.

REFERENCES

1. Deng, Y., Ma, L., and Mao, Y. (2016). Biological production of adipic acid from renewable substrates: current and future methods. Biochem. Eng. J. *105*, 16–26. https://doi.org/10.1016/j.bej.2015.08.015.
2. Schutyser, W., Van den Bosch, S., Dijkmans, J., Turner, S., Meledina, M., Van Tendeloo, G., Debecker, D.P., and Sels, B.F. (2015). Selective nickel-catalyzed conversion of model and lignin-derived phenolic compounds to cyclohexanone-based polymer building blocks. ChemSusChem *8*, 1805–1818. https://doi.org/10.1002/cssc.201403375.
3. Zhu, C., Cao, J.-P., Zhao, X.-Y., Xie, T., Ren, J., and Wei, X.-Y. (2019). Mechanism of Ni-catalyzed selective CO cleavage of lignin model compound benzyl phenyl ether under mild conditions. J. Energy Inst. *92*, 74–81. https://doi.org/10.1016/j.joei.2017.11.004.
4. Yong, K.J., and Wu, T.Y. (2023). Recent advances in the application of alcohols in extracting lignin with preserved β-O-4 content from lignocellulosic biomass. Bioresour. Technol. *384*, 129238. https://doi.org/10.1016/j.biortech.2023.129238.
5. Long, J., Shu, S., Wu, Q., Yuan, Z., Wang, T., Xu, Y., Zhang, X., Zhang, Q., and Ma, L. (2015). Selective cyclohexanol production from the renewable lignin derived phenolic chemicals catalyzed by Ni/MgO. Energy Convers. Manag. *105*, 570–577. https://doi.org/10.1016/j.enconman.2015.08.016.
6. Lu, M., Jiang, Y., Sun, Y., Zhang, P., Zhu, J., Li, M., Shan, Y., Shen, J., and Song, C. (2020). Hydrodeoxygenation of guaiacol catalyzed by ZrO2–CeO2-Supported nickel catalysts with high loading. Energy Fuels *34*, 4685–4692. https://doi.org/10.1021/acs.energyfuels.0c00445.
7. Long, W., Liu, P., Xiong, W., Hao, F., and Luo, H.a. (2020). Conversion of guaiacol as lignin model component using acid-treated, multi-walled carbon nanotubes supported Ru–MnO bimetallic catalysts. Can. J. Chem. *98*, 57–65. https://doi.org/10.1139/cjc-2019-0261.
8. Dongil, A.B., Ghampson, I.T., García, R., Fierro, J.L.G., and Escalona, N. (2016). Hydrodeoxygenation of guaiacol over Ni/carbon catalysts: effect of the support and Ni loading. RSC Adv. *6*, 2611–2623. https://doi.org/10.1039/C5RA22540J.
9. Guo, Z., Zhang, Q., You, T., Zhang, X., Xu, F., and Wu, Y. (2019). Short-time deep eutectic solvent pretreatment for enhanced enzymatic saccharification and lignin valorization. Green Chem. *21*, 3099–3108. https://doi.org/10.1039/C9GC00704K.
10. Tong, Y., Yang, T., Wang, J., Li, B., Zhai, Y., and Li, R. (2024). A review on the overall process of lignin to phenolic compounds for chemicals and fuels: from separation and extraction of lignin to transformation. J. Anal. Appl. Pyrol. *181*, 106663. https://doi.org/10.1016/j.jaap.2024.106663.
11. Chen, X., Mosier, N., and Ladisch, M. (2024). Valorization of lignin from aqueous-based lignocellulosic biorefineries. Trends Biotechnol. *42*, 1348–1362. https://doi.org/10.1016/j.tibtech.2024.07.004.
12. Liu, X., Bouxin, F.P., Fan, J., Budarin, V.L., Hu, C., and Clark, J.H. (2020). Recent advances in the catalytic depolymerization of lignin towards phenolic chemicals: a review. ChemSusChem *13*, 4296–4317. https://doi.org/10.1002/cssc.202001213.
13. Van den Bosch, S., Schutyser, W., Vanholme, R., Driessen, T., Koelewijn, S.-F., Renders, T., De Meester, B., Huijgen, W.J.J., Dehaen, W., Courtin, C.M., et al. (2015). Reductive lignocellulose fractionation into soluble lignin-derived phenolic monomers and dimers and processable carbohydrate pulps. Energy Environ. Sci. *8*, 1748–1763. https://doi.org/10.1039/C5EE00204D.
14. Jing, Y., Dong, L., Guo, Y., Liu, X., and Wang, Y. (2020). Chemicals from lignin: a review of catalytic conversion involving hydrogen. ChemSusChem *13*, 4181–4198. https://doi.org/10.1002/cssc.201903174.
15. Chen, M.-Y., Huang, Y.-B., Pang, H., Liu, X.-X., and Fu, Y. (2015). Hydrodeoxygenation of lignin-derived phenols into alkanes over carbon nanotube supported Ru catalysts in biphasic systems. Green Chem. *17*, 1710–1717. https://doi.org/10.1039/C4GC01992J.
16. Hong, Y.-K., Lee, D.-W., Eom, H.-J., and Lee, K.-Y. (2014). The catalytic activity of Pd/WOx/γ-Al2O3 for hydrodeoxygenation of guaiacol. Appl. Cat. B *150–151*, 438–445. https://doi.org/10.1016/j.apcatb.2013.12.045.
17. Hellinger, M., Carvalho, H.W.P., Baier, S., Wang, D., Kleist, W., and Grunwaldt, J.-D. (2015). Catalytic hydrodeoxygenation of guaiacol over platinum supported on metal oxides and zeolites. Appl. Cat. A *490*, 181–192. https://doi.org/10.1016/j.apcata.2014.10.043.
18. De Castro, I.B.D., Graça, I., Rodríguez-García, L., Kennema, M., Rinaldi, R., and Meemken, F. (2018). Elucidating the reactivity of methoxyphenol positional isomers towards hydrogen-transfer reactions by ATR-IR spectroscopy of the liquid–solid interface of RANEY® Ni. Catal. Sci. Technol. *8*, 3107–3114. https://doi.org/10.1039/C8CY00491A.
19. Mochizuki, T., Chen, S.-Y., Toba, M., and Yoshimura, Y. (2014). Deoxygenation of guaiacol and woody tar over reduced catalysts. Appl. Cat. B *146*, 237–243. https://doi.org/10.1016/j.apcatb.2013.05.040.
20. Liu, X., Jia, W., Xu, G., Zhang, Y., and Fu, Y. (2017). Selective hydrodeoxygenation of lignin-derived phenols to cyclohexanols over co-based catalysts. ACS Sustainable Chem. Eng. *5*, 8594–8601. https://doi.org/10.1021/acssuschemeng.7b01047.
21. Leiva, K., Martinez, N., Sepulveda, C., García, R., Jiménez, C.A., Laurenti, D., Vrinat, M., Geantet, C., Fierro, J.L.G., Ghampson, I.T., et al. (2015). Hydrodeoxygenation of 2-methoxyphenol over different Re active phases supported on SiO2 catalysts. Appl. Cat. A *490*, 71–79. https://doi.org/10.1016/j.apcata.2014.10.054.
22. Yi, J., Luo, Y., He, T., Jiang, Z., Li, J., and Hu, C. (2016). High efficient hydrogenation of lignin-derived monophenols to cyclohexanols over Pd/γ-Al2O3 under mild conditions. Catalysts *6*, 12. https://doi.org/10.3390/catal6010012.
23. Roldugina, E.A., Naranov, E.R., Maximov, A.L., and Karakhanov, E.A. (2018). Hydrodeoxygenation of guaiacol as a model compound of bio-oil in methanol over mesoporous noble metal catalysts. Appl. Cat. A *553*, 24–35. https://doi.org/10.1016/j.apcata.2018.01.008.
24. Zhou, H., Wang, H., Sadow, A.D., and Slowing, I.I. (2020). Toward hydrogen economy: selective guaiacol hydrogenolysis under ambient hydrogen pressure. Appl. Cat. B *270*, 118890. https://doi.org/10.1016/j.apcatb.2020.118890.
25. He, Z., Hu, M., and Wang, X. (2018). Highly effective hydrodeoxygenation of guaiacol on Pt/TiO2: promoter effects. Cat. Today *302*, 136–145. https://doi.org/10.1016/j.cattod.2017.02.034.
26. Mao, J., Zhou, J., Xia, Z., Wang, Z., Xu, Z., Xu, W., Yan, P., Liu, K., Guo, X., and Zhang, Z.C. (2017). Anatase TiO2 activated by gold nanoparticles for selective hydrodeoxygenation of guaiacol to phenolics. ACS Cat. *7*, 695–705. https://doi.org/10.1021/acscatal.6b02368.
27. Wang, X., Zhang, Z., Yan, Z., Li, Q., and Zhang, Y. (2023). Catalysts with metal-acid dual sites for selective hydrodeoxygenation of lignin derivatives: progress in regulation strategies and applications. Appl. Cat. A *662*, 119266. https://doi.org/10.1016/j.apcata.2023.119266.
28. Ouedraogo, A.S., and Bhoi, P.R. (2020). Recent progress of metals supported catalysts for hydrodeoxygenation of biomass derived pyrolysis oil. J. Cleaner Prod. *253*, 119957. https://doi.org/10.1016/j.jclepro.2020.119957.
29. Betsy, K.J., Lazar, A., and Vinod, C.P. (2018). Highly selective aqueous phase hydrogenation of phenols over nanostructured RuO2 on

MCM-41 catalysts. Nano Struct. Nano Objects *13*, 36–43. https://doi.org/10.1016/j.nanoso.2017.11.004.

30. Jung, K.B., Lee, J., Ha, J.-M., Lee, H., Suh, D.J., Jun, C.-H., and Jae, J. (2018). Effective hydrodeoxygenation of lignin-derived phenols using bimetallic RuRe catalysts: effect of carbon supports. Cat. Today *303*, 191–199. https://doi.org/10.1016/j.cattod.2017.07.027.
31. Kim, M., Ha, J.-M., Lee, K.-Y., and Jae, J. (2016). Catalytic transfer hydrogenation/hydrogenolysis of guaiacol to cyclohexane over bimetallic RuRe/C catalysts. Cat. Commun. *86*, 113–118. https://doi.org/10.1016/j.catcom.2016.08.022.
32. Dwiatmoko, A.A., Zhou, L., Kim, I., Choi, J.-W., Suh, D.J., and Ha, J.-M. (2016). Hydrodeoxygenation of lignin-derived monomers and lignocellulose pyrolysis oil on the carbon-supported Ru catalysts. Cat. Today *265*, 192–198. https://doi.org/10.1016/j.cattod.2015.08.027.
33. Zhou, H., Wang, H., Perras, F.A., Naik, P., Pruski, M., Sadow, A.D., and Slowing, I.I. (2020). Two-step conversion of Kraft lignin to nylon precursors under mild conditions. Green Chem. *22*, 4676–4682. https://doi.org/10.1039/D0GC01220C.
34. Chang, J., Danuthai, T., Dewiyanti, S., Wang, C., and Borgna, A. (2013). Hydrodeoxygenation of guaiacol over carbon-supported metal catalysts. ChemCatChem *5*, 3041–3049. https://doi.org/10.1002/cctc.201300096.
35. Luo, B., Li, R., Shu, R., Wang, C., Zhang, J., and Chen, Y. (2020). Boric acid as a novel homogeneous catalyst coupled with Ru/C for hydrodeoxygenation of phenolic compounds and raw lignin oil. Ind. Eng. Chem. Res. *59*, 17192–17199. https://doi.org/10.1021/acs.iecr.0c00888.
36. Gao, D., Schweitzer, C., Hwang, H.T., and Varma, A. (2014). Conversion of guaiacol on noble metal catalysts: reaction performance and deactivation studies. Ind. Eng. Chem. Res. *53*, 18658–18667. https://doi.org/10.1021/ie500495z.
37. Nakagawa, Y., Ishikawa, M., Tamura, M., and Tomishige, K. (2014). Selective production of cyclohexanol and methanol from guaiacol over Ru catalyst combined with MgO. Green Chem. *16*, 2197–2203. https://doi.org/10.1039/C3GC42322K.
38. Ishikawa, M., Tamura, M., Nakagawa, Y., and Tomishige, K. (2016). Demethoxylation of guaiacol and methoxybenzenes over carbon-supported Ru–Mn catalyst. Appl. Cat. B *182*, 193–203. https://doi.org/10.1016/j.apcatb.2015.09.021.
39. Xu, G.-Y., Guo, J.-H., Qu, Y.-C., Zhang, Y., Fu, Y., and Guo, Q.-X. (2016). Selective hydrodeoxygenation of lignin-derived phenols to alkyl cyclohexanols over a Ru-solid base bifunctional catalyst. Green Chem. *18*, 5510–5517. https://doi.org/10.1039/C6GC01097K.
40. Singh, D., and Dhepe, P.L. (2020). Understanding the influence of alumina supported ruthenium catalysts synthesis and reaction parameters on the hydrodeoxygenation of lignin derived monomers. Mol. Cat. *480*, 110525. https://doi.org/10.1016/j.mcat.2019.110525.
41. Han, B., Bao, Z., Liu, T., Zhou, H., Zhuang, G., Zhong, X., Deng, S., and Wang, J. (2017). Enhanced catalytic performances for guaiacol aqueous phase hydrogenation over ruthenium supported on mesoporous TiO2 hollow spheres embedded with SiO2 nanoparticles. ChemistrySelect *2*, 9599–9606. https://doi.org/10.1002/slct.201702013.
42. Zhang, K., Meng, Q., Wu, H., Yan, J., Mei, X., An, P., Zheng, L., Zhang, J., He, M., and Han, B. (2022). Selective hydrodeoxygenation of aromatics to cyclohexanols over Ru Single atoms supported on CeO2. J. Am. Chem. Soc. *144*, 20834–20846. https://doi.org/10.1021/jacs.2c08992.
43. Sun, H., Ding, Y., Duan, J., Zhang, Q., Wang, Z., Lou, H., and Zheng, X. (2010). Transesterification of sunflower oil to biodiesel on ZrO2 supported La2O3 catalyst. Bioresour. Technol. *101*, 953–958. https://doi.org/10.1016/j.biortech.2009.08.089.
44. Salinas, D., Escalona, N., Pecchi, G., and Fierro, J.L.G. (2019). Lanthanum oxide behavior in La2O3-Al2O3 and La2O3-ZrO2 catalysts with application in FAME production. Fuel *253*, 400–408. https://doi.org/10.1016/j.fuel.2019.05.015.
45. Khan, T.S., Singh, D., Samal, P.P., Krishnamurty, S., and Dhepe, P.L. (2021). Mechanistic investigations on the catalytic transfer hydrogenation of lignin-derived monomers over Ru catalysts: theoretical and kinetic studies. ACS Sustainable Chem. Eng. *9*, 14040–14050. https://doi.org/10.1021/acssuschemeng.1c02942.
46. Nie, R., Yang, H., Zhang, H., Yu, X., Lu, X., Zhou, D., and Xia, Q. (2017). Mild-temperature hydrodeoxygenation of vanillin over porous nitrogen-doped carbon black supported nickel nanoparticles. Green Chem. *19*, 3126–3134. https://doi.org/10.1039/C7GC00531H.
47. Jiang, H., Yu, X., Peng, X., Zhang, H., Nie, R., Lu, X., Zhou, D., and Xia, Q. (2016). Efficient aqueous hydrodeoxygenation of vanillin over a mesoporous carbon nitride-modified Pd nanocatalyst. RSC Adv. *6*, 69045–69051. https://doi.org/10.1039/C6RA11851H.
48. Liu, Y., Wu, X., Li, Z., Zhang, J., Liu, S.-X., Liu, S., Gu, L., Zheng, L.R., Li, J., Wang, D., et al. (2021). Fabricating polyoxometalates-stabilized single-atom site catalysts in confined space with enhanced activity for alkynes diboration. Nat. Commun. *12*, 4205. https://doi.org/10.1038/s41467-021-24513-x.
49. Chen, H., and Sun, J. (2021). Selective hydrogenation of phenol for cyclohexanone: a review. J. Ind. Eng. Chem. *94*, 78–91. https://doi.org/10.1016/j.jiec.2020.11.022.
50. Song, W., He, Y., Lai, S., Lai, W., Yi, X., Yang, W., and Jiang, X. (2020). Selective hydrodeoxygenation of lignin phenols to alcohols in the aqueous phase over a hierarchical Nb 2 O 5-supported Ni catalyst. Green Chem. *22*, 1662–1670. https://doi.org/10.1039/C9GC03842F.
51. Lu, J., Liu, X., Yu, G., Lv, J., Rong, Z., Wang, M., and Wang, Y. (2020). Selective hydrodeoxygenation of guaiacol to cyclohexanol catalyzed by nanoporous nickel. Cat. Lett. *150*, 837–848. https://doi.org/10.1007/s10562-019-02967-5.
52. Escalona, N., Aranzaez, W., Leiva, K., Martínez, N., and Pecchi, G. (2014). Ni nanoparticles prepared from ce substituted LaNiO3 for the guaiacol conversion. Appl. Cat. A *481*, 1–10. https://doi.org/10.1016/j.apcata.2014.04.037.
53. Cui, X., Yuan, H., Junge, K., Topf, C., Beller, M., and Shi, F. (2017). A stable and practical nickel catalyst for the hydrogenolysis of C–O bonds. Green Chem. *19*, 305–310. https://doi.org/10.1039/C6GC01955B.
54. Shu, R., Zhang, Q., Xu, Y., Long, J., Ma, L., Wang, T., Chen, P., and Wu, Q. (2016). Hydrogenation of lignin-derived phenolic compounds over step by step precipitated Ni/SiO 2. RSC Adv. *6*, 5214–5222. https://doi.org/10.1039/C5RA23041A.
55. López, M., Palacio, R., Royer, S., Mamede, A.-S., and Fernández, J.J. (2020). Mesostructured CMK-3 carbon supported Ni–ZrO_2 as catalysts for the hydrodeoxygenation of guaiacol. Micropor. Mesopor. Mater. *292*, 109694. https://doi.org/10.1016/j.micromeso.2019.109694.
56. Wang, X., and Rinaldi, R. (2012). Exploiting H-transfer reactions with RANEY® Ni for upgrade of phenolic and aromatic biorefinery feeds under unusual, low-severity conditions. Energy Environ. Sci. *5*, 8244–8260. https://doi.org/10.1039/c2ee21855k.
57. Yang, Q., Liu, G., and Liu, Y. (2018). Perovskite-type oxides as the catalyst precursors for preparing supported metallic nanocatalysts: a review. Ind. Eng. Chem. Res. *57*, 1–17. https://doi.org/10.1021/acs.iecr.7b03251.
58. Hu, S., Xue, M., Chen, H., and Shen, J. (2010). The effect of surface acidic and basic properties on the hydrogenation of aromatic rings over the supported nickel catalysts. Chem. Eng. J. *162*, 371–379. https://doi.org/10.1016/j.cej.2010.05.019.
59. Verma, D., Insyani, R., Cahyadi, H.S., Park, J., Kim, S.M., Cho, J.M., Bae, J.W., and Kim, J. (2018). Ga-doped Cu/H-nanozeolite-Y catalyst for selective hydrogenation and hydrodeoxygenation of lignin-derived chemicals. Green Chem. *20*, 3253–3270. https://doi.org/10.1039/C8GC00629F.
60. Grau-Crespo, R., de Leeuw, N.H., Hamad, S., and Waghmare, U.V. (2011). Phase separation and surface segregation in ceria–zirconia solid

solutions. Proc. R. Soc. A. *467*, 1925–1938. https://doi.org/10.1098/rspa.2010.0512.

61. Wang, X., Arai, M., Wu, Q., Zhang, C., and Zhao, F. (2020). Hydrodeoxygenation of lignin-derived phenolics–a review on the active sites of supported metal catalysts. Green Chem. *22*, 8140–8168. https://doi.org/10.1039/D0GC02610G.
62. Liu, X., Xu, L., Xu, G., Jia, W., Ma, Y., and Zhang, Y. (2016). Selective hydrodeoxygenation of lignin-derived phenols to cyclohexanols or cyclohexanes over magnetic CoNx@NC catalysts under mild conditions. ACS Cat. *6*, 7611–7620. https://doi.org/10.1021/acscatal.6b01785.
63. Song, Q.-L., Zhao, Y.-P., Wu, F.-P., Li, G.-S., Fan, X., Wang, R.-Y., Cao, J.-P., and Wei, X.-Y. (2020). Selective hydrogenolysis of lignin-derived aryl ethers over Co/C@ N catalysts. Renew. Energy *148*, 729–738. https://doi.org/10.1016/j.renene.2019.10.160.
64. Wang, B., Zhou, P., Yan, X., Li, H., Wu, H., and Zhang, Z. (2023). Cooperative catalysis of Co single atoms and nanoparticles enables selective CAr−OCH3 cleavage for sustainable production of lignin-based cyclohexanols. J. Energy Chem. *79*, 535–549. https://doi.org/10.1016/j.jechem.2022.12.020.
65. Wei, J., Zhou, D., Sun, Z., Deng, Y., Xia, Y., and Zhao, D. (2013). A controllable synthesis of rich nitrogen-doped ordered mesoporous carbon for CO2 capture and supercapacitors. Adv. Funct. Mater. *23*, 2322–2328. https://doi.org/10.1002/adfm.201202764.
66. Meng, Z., Qiu, Z., Shi, Y., Wang, S., Zhang, G., Pi, Y., and Pang, H. (2023). Micro/Nano Metal–Organic Frameworks Meet Energy Chemistry: A Review of Materials Synthesis and Applications. eScience *3*, 100092.
67. Alonso, D.M., Wettstein, S.G., and Dumesic, J.A. (2012). Bimetallic catalysts for upgrading of biomass to fuels and chemicals. Chem. Soc. Rev. *41*, 8075–8098. https://doi.org/10.1039/c2cs35188a.
68. Li, C., Zhao, X., Wang, A., Huber, G.W., and Zhang, T. (2015). Catalytic transformation of lignin for the production of chemicals and fuels. Chem. Rev. *115*, 11559–11624. https://doi.org/10.1021/acs.chemrev.5b00155.
69. Xu, H., Ju, J., and Li, H. (2022). Toward efficient heterogeneous catalysts for in-situ hydrodeoxygenation of biomass. Fuel *320*, 123891. https://doi.org/10.1016/j.fuel.2022.123891.
70. Feng, W., Yang, L., Cao, N., Du, C., Dai, H., Luo, W., and Cheng, G. (2014). In situ facile synthesis of bimetallic CoNi catalyst supported on graphene for hydrolytic dehydrogenation of amine borane. Int. J. Hydrog. Energy *39*, 3371–3380. https://doi.org/10.1016/j.ijhydene.2013.12.113.
71. Huang, C., Zhang, H., Zhao, Y., Chen, S., and Liu, Z. (2012). Diatomite-supported Pd–M (M= Cu, Co, Ni) bimetal nanocatalysts for selective hydrogenation of long-chain aliphatic esters. J. Colloid Interface Sci. *386*, 60–65. https://doi.org/10.1016/j.jcis.2012.07.032.
72. Hou, W., Dehm, N.A., and Scott, R.W. (2008). Alcohol oxidations in aqueous solutions using Au, Pd, and bimetallic AuPd nanoparticle catalysts. J. Cat. *253*, 22–27. https://doi.org/10.1016/j.jcat.2007.10.025.
73. Huynh, T.M., Armbruster, U., Pohl, M.M., Schneider, M., Radnik, J., Hoang, D.L., Phan, B.M.Q., Nguyen, D.A., and Martin, A. (2014). Hydrodeoxygenation of phenol as a model compound for bio-oil on non-noble bimetallic nickel-based catalysts. ChemCatChem *6*, 1940–1951. https://doi.org/10.1002/cctc.201402011.
74. Zhou, M., Ye, J., Liu, P., Xu, J., and Jiang, J. (2017). Water-assisted selective hydrodeoxygenation of guaiacol to cyclohexanol over supported Ni and Co bimetallic catalysts. ACS Sustainable Chem. Eng. *5*, 8824–8835. https://doi.org/10.1021/acssuschemeng.7b01615.
75. Chen, C., Zhou, M., Liu, P., Sharma, B.K., and Jiang, J. (2020). Flexible NiCo-based catalyst for direct hydrodeoxygenation of guaiacol to cyclohexanol. New J. Chem. *44*, 18906–18916. https://doi.org/10.1039/D0NJ02929G.
76. Xu, Q., Shi, Y., Yang, L., Fan, G., and Li, F. (2020). The promotional effect of surface Ru decoration on the catalytic performance of Co-based nanocatalysts for guaiacol hydrodeoxygenation. Mol. Cat. *497*, 111224. https://doi.org/10.1016/j.mcat.2020.111224.
77. Zhao, M., Hu, J., Wu, S., Yang, L., An, X., Yuan, P., and Lu, P. (2022). Hydrodeoxygenation of lignin-derived phenolics over facile prepared bimetallic RuCoNx/NC. Fuel *308*, 121979. https://doi.org/10.1016/j.fuel.2021.121979.
78. Tong, L., Cai, B., Zhang, R., Feng, J., and Pan, H. (2021). In situ hydrodeoxygenation of lignin-derived phenols with synergistic effect between the bimetal and Nb2O5 support. Front. Energy Res. *9*. https://doi.org/10.3389/fenrg.2021.746109.
79. Saleheen, M., Verma, A.M., Mamun, O., Lu, J., and Heyden, A. (2019). Investigation of solvent effects on the hydrodeoxygenation of guaiacol over Ru catalysts. Catal. Sci. Technol. *9*, 6253–6273. https://doi.org/10.1039/C9CY01763A.
80. Deng, W., Feng, Y., Fu, J., Guo, H., Guo, Y., Han, B., Jiang, Z., Kong, L., Li, C., and Liu, H. (2022). Catalytic conversion of lignocellulosic biomass into chemicals and fuels. Green Energy Environ. *8*, 10–114.
81. Hellinger, M., Carvalho, H.W.P.d., Baier, S., Gharnati, L., and Grunwaldt, J.D. (2015). Solvent influence on the hydrodeoxygenation of guaiacol over Pt/SiO2 and Pt/H-MFI 90 catalysts. Chem. Ing. Tech. *87*, 1771–1780. https://doi.org/10.1002/cite.201500143.
82. Yoon, J.S., Choi, J.W., Suh, D.J., Lee, K., Lee, H., and Ha, J.M. (2015). Water-assisted selective hydrodeoxygenation of lignin-derived guaiacol to monooxygenates. ChemCatChem *7*, 2669–2674. https://doi.org/10.1002/cctc.201500345.
83. Liu, G.-H., Zong, Z.-M., Liu, Z.-Q., Liu, F.-J., Zhang, Y.-Y., and Wei, X.-Y. (2018). Solvent-controlled selective hydrodeoxygenation of bio-derived guaiacol to arenes or phenols over a biochar supported Co-doped MoO2 catalyst. Fuel Process. Technol. *179*, 114–123. https://doi.org/10.1016/j.fuproc.2018.05.035.
84. Wan, H., Chaudhari, R.V., and Subramaniam, B. (2012). Catalytic hydroprocessing of p-cresol: metal, solvent and mass-transfer effects. Top. Cat. *55*, 129–139. https://doi.org/10.1007/s11244-012-9782-6.
85. Hensley, A.J.R., Bray, J., Shangguan, J., Chin, Y.-H.C., and McEwen, J.-S. (2021). Catalytic consequences of hydrogen addition events and solvent-adsorbate interactions during guaiacol-H2 reactions at the H2O-Ru (0 0 0 1) interface. J. Cat. *395*, 467–482. https://doi.org/10.1016/j.jcat.2020.09.034.
86. Schutyser, W., Van den Bossche, G., Raaffels, A., Van den Bosch, S., Koelewijn, S.-F., Renders, T., and Sels, B.F. (2016). Selective conversion of lignin-derivable 4-alkylguaiacols to 4-alkylcyclohexanols over noble and non-noble-metal catalysts. ACS Sustainable Chem. Eng. *4*, 5336–5346. https://doi.org/10.1021/acssuschemeng.6b01580.
87. Cai, B., Zhou, X.-C., Miao, Y.-C., Luo, J.-Y., Pan, H., and Huang, Y.-B. (2017). Enhanced catalytic transfer hydrogenation of ethyl levulinate to γ-valerolactone over a robust Cu–Ni bimetallic catalyst. ACS Sustainable Chem. Eng. *5*, 1322–1331. https://doi.org/10.1021/acssuschemeng.6b01677.
88. Kuwahara, Y., Kaburagi, W., and Fujitani, T. (2014). Catalytic transfer hydrogenation of levulinate esters to γ-valerolactone over supported ruthenium hydroxide catalysts. RSC Adv. *4*, 45848–45855. https://doi.org/10.1039/C4RA08074B.
89. Xu, H., and Li, H. (2022). Alcohol-assisted hydrodeoxygenation as a sustainable and cost-effective pathway for biomass derivatives upgrading. J. Energy Chem. *73*, 133–159. https://doi.org/10.1016/j.jechem.2022.05.021.
90. Gollakota, A.R.K., Reddy, M., Subramanyam, M.D., and Kishore, N. (2016). A review on the upgradation techniques of pyrolysis oil. Renew. Sustain. Energy Rev. *58*, 1543–1568. https://doi.org/10.1016/j.rser.2015.12.180.
91. Huang, L., Tang, F., Liu, P., Xiong, W., Jia, S., Hao, F., Lv, Y., and Luo, H. (2022). Highly efficient and selective conversion of guaiacol to cyclohexanol over Ni-Fe/MgAlOx: understanding the synergistic effect between

Ni-Fe alloy and basic sites. Fuel *327*, 125115. https://doi.org/10.1016/j.fuel.2022.125115.

92. Li, H., Ma, H., Zhao, W., Li, X., and Long, J. (2019). Upgrading lignin bio-oil for oxygen-containing fuel production using Ni/MgO: effect of the catalyst calcination temperature. Appl. Energy *253*, 113613. https://doi.org/10.1016/j.apenergy.2019.113613.
93. Hu, X., Zhang, Z., Gholizadeh, M., Zhang, S., Lam, C.H., Xiong, Z., and Wang, Y. (2020). Coke formation during thermal treatment of bio-oil. Energy Fuels *34*, 7863–7914. https://doi.org/10.1021/acs.energyfuels.0c01323.
94. Latifi, E., Marchese, A.D., Hulls, M.C.W., Soldatov, D.V., and Schlaf, M. (2017). [Ru(triphos)(CH 3 CN) 3](OTf) 2 as a homogeneous catalyst for the hydrogenation of biomass derived 2,5-hexanedione and 2,5-dimethyl-furan in aqueous acidic medium. Green Chem. *19*, 4666–4679. https://doi.org/10.1039/C7GC01956D.
95. Bykova, M.V., Ermakov, D.Y., Kaichev, V.V., Bulavchenko, O.A., Saraev, A.A., Lebedev, M.Y., and Yakovlev, V.A. (2012). Ni-based sol–gel catalysts as promising systems for crude bio-oil upgrading: guaiacol hydrodeoxygenation study. Appl. Cat. B *113–114*, 296–307. https://doi.org/10.1016/j.apcatb.2011.11.051.
96. Qi, S.-C., Zhang, L., Einaga, H., Kudo, S., Norinaga, K., and Hayashi, J.-i. (2017). Nano-sized nickel catalyst for deep hydrogenation of lignin monomers and first-principles insight into the catalyst preparation. J. Mater. Chem. A *5*, 3948–3965. https://doi.org/10.1039/C6TA08538E.
97. Imbihl, R., and Ertl, G. (1995). Oscillatory kinetics in heterogeneous catalysis. Chem. Rev. *95*, 697–733. https://doi.org/10.1021/cr00035a012.
98. Chen, W., Luo, Z., Yu, C., Yang, Y., Li, G., and Zhang, J. (2014). Catalytic conversion of guaiacol in ethanol for bio-oil upgrading to stable oxygenated organics. Fuel Process. Technol. *126*, 420–428. https://doi.org/10.1016/j.fuproc.2014.05.022.
99. Song, W., Liu, Y., Baráth, E., Zhao, C., and Lercher, J.A. (2015). Synergistic effects of Ni and acid sites for hydrogenation and C–O bond cleavage of substituted phenols. Green Chem. *17*, 1204–1218. https://doi.org/10.1039/C4GC01798F.
100. Bjelić, A., Grilc, M., and Likozar, B. (2018). Catalytic hydrogenation and hydrodeoxygenation of lignin-derived model compound eugenol over Ru/C: intrinsic microkinetics and transport phenomena. Chem. Eng. J. *333*, 240–259. https://doi.org/10.1016/j.cej.2017.09.135.
101. Karakhanov, E.A., Boronoev, M.P., Filippova, T.Y., and Maksimov, A.L. (2018). Guaiacol hydrogenation in an aqueous medium in the presence of a palladium catalyst supported on a mesoporous dendrimer-containing polymer. Petrol. Chem. *58*, 407–411. https://doi.org/10.1134/S0965544118050080.
102. Gutierrez, A., Kaila, R.K., Honkela, M.L., Slioor, R., and Krause, A.O.I. (2009). Hydrodeoxygenation of guaiacol on noble metal catalysts. Cat. Today *147*, 239–246. https://doi.org/10.1016/j.cattod.2008.10.037.
103. Phan, D.-P., Vo, T.K., Le, V.N., Kim, J., and Lee, E.Y. (2020). Spray pyrolysis synthesis of bimetallic NiMo/Al2O3–TiO2 catalyst for hydrodeoxygenation of guaiacol: effects of bimetallic composition and reduction temperature. J. Ind. Eng. Chem. *83*, 351–358. https://doi.org/10.1016/j.jiec.2019.12.008.
104. He, Y., Bie, Y., Lehtonen, J., Liu, R., and Cai, J. (2019). Hydrodeoxygenation of guaiacol as a model compound of lignin-derived pyrolysis bio-oil over zirconia-supported Rh catalyst: process optimization and reaction kinetics. Fuel *239*, 1015–1027. https://doi.org/10.1016/j.fuel.2018.11.103.
105. Bjelić, A., Grilc, M., Huš, M., and Likozar, B. (2019). Hydrogenation and hydrodeoxygenation of aromatic lignin monomers over Cu/C, Ni/C, Pd/C, Pt/C, Rh/C and Ru/C catalysts: mechanisms, reaction micro-kinetic modelling and quantitative structure-activity relationships. Chem. Eng. J. *359*, 305–320. https://doi.org/10.1016/j.cej.2018.11.107.
106. Hensley, A.J.R., Wang, Y., and McEwen, J.-S. (2016). Adsorption of guaiacol on Fe (110) and Pd (111) from first principles. Surf. Sci. *648*, 227–235. https://doi.org/10.1016/j.susc.2015.10.030.